



## Jasmonate signaling controls negative and positive effectors of salt stress tolerance in rice

Simon Ndecky, Elisabeth Eiche, Valérie Cognat, David Pflieger, Nitin Pawar, Ferdinand Betting, Somidh Saha, Antony Champion, Michael Riemann, Thierry Heitz, et al.

### ► To cite this version:

Simon Ndecky, Elisabeth Eiche, Valérie Cognat, David Pflieger, Nitin Pawar, et al.. Jasmonate signaling controls negative and positive effectors of salt stress tolerance in rice. *Journal of Experimental Botany*, 2023, 74 (10), pp.3220-3239. 10.1093/jxb/erad086 . hal-04266591

**HAL Id: hal-04266591**

**<https://hal.science/hal-04266591v1>**

Submitted on 31 Oct 2023

**HAL** is a multi-disciplinary open access archive for the deposit and dissemination of scientific research documents, whether they are published or not. The documents may come from teaching and research institutions in France or abroad, or from public or private research centers.

L'archive ouverte pluridisciplinaire **HAL**, est destinée au dépôt et à la diffusion de documents scientifiques de niveau recherche, publiés ou non, émanant des établissements d'enseignement et de recherche français ou étrangers, des laboratoires publics ou privés.



**Jasmonate signaling controls negative and positive effectors of salt stress tolerance in rice**

Simon Ndecky<sup>1</sup>, Trang Hieu Nguyen<sup>2</sup>, Elisabeth Eiche<sup>3</sup>, Valérie Cognat<sup>1</sup>, David Pflieger<sup>1</sup>, Nitin Pawar<sup>4</sup>, Ferdinand Betting<sup>5</sup>, Somidh Saha<sup>5</sup>, Antony Champion<sup>2</sup>, Michael Riemann<sup>4</sup> and Thierry Heitz<sup>1\*</sup>

<sup>1</sup> Institut de Biologie Moléculaire des Plantes (IBMP) du CNRS, Université de Strasbourg, Strasbourg, France

<sup>2</sup> DIADE, Institut de Recherche et de Développement (IRD), Université de Montpellier, Montpellier, France

<sup>3</sup> Institute for Applied Geosciences, Karlsruhe Institute of Technology (KIT), Karlsruhe, Germany

<sup>4</sup> Botanical Institute, Karlsruhe Institute of Technology (KIT), Karlsruhe, Germany

<sup>5</sup> Institute for Technology Assessment and Systems Analysis (ITAS), Karlsruhe Institute of Technology (KIT), Karlsruhe, Germany

**\*Correspondance**

Thierry Heitz, Institut de Biologie Moléculaire des Plantes (IBMP) du CNRS, Université de Strasbourg, Strasbourg, France

E-mail : [thierry.heitz@ibmp-cnrs.unistra.fr](mailto:thierry.heitz@ibmp-cnrs.unistra.fr); ORCID: [0000-0001-6238-8264](https://orcid.org/0000-0001-6238-8264)

**Running head:** The jasmonate-dependent components of salt-stress response in rice



## Highlight

Jasmonate dually impacts osmotic and ionic components of salt stress in rice. Jasmonate is required for abscisic acid-mediated water deprivation responses, but inhibits Na<sup>+</sup> retention in roots, promoting leaf damage.

## Abstract

Plant responses to salt exposure involve large reconfiguration of hormonal pathways that orchestrate physiological changes towards tolerance. Jasmonate (JA) hormones are essential to withstand biotic and abiotic assaults, but their roles in salt tolerance remain unclear. Here we describe the dynamics of JA metabolism and signaling in root and leaf of rice, a plant species that is highly exposed and sensitive to salt. Roots activate the JA pathway in an early pulse, while 2<sup>nd</sup> leaf displays a biphasic JA response with peaks at 1 hour and 3 days post-exposure. Based on higher salt tolerance of a rice JA-deficient mutant (*aoc*), we examined through kinetic transcriptome and physiological analysis the salt-triggered processes that are under JA control. Profound genotype-differential features emerged that could underlie observed phenotypes. ABA content and ABA-dependent water deprivation responses were impaired in *aoc* shoots. Moreover, *aoc* accumulated more Na<sup>+</sup> in roots, and less in leaf, with reduced ion translocation correlating with root derepression of the *HAK4* Na<sup>+</sup> transporter. Distinct reactive oxygen species scavengers were also stronger in *aoc* leaf, along with reduced senescence and chlorophyll catabolism markers. Collectively, the data identify contrasted contributions of JA signaling to different sectors of the salt stress response in rice.

**Keywords:** jasmonate, rice, salt stress, signaling, tolerance, transcriptome



## 1. INTRODUCTION

Upcoming global climate perturbations are imposing more frequent stressful conditions to plants, including flood, drought, or extreme temperatures episodes. Soil salinization adds as an increasing limiting factor to crop productivity in coastal agricultural areas, causing growth retardation and yield losses. Rice (*Oryza sativa*), the major staple food crop for more than half of the world's population, is particularly exposed to stress and due to its uppermost importance for food security, has been established as a model species for monocotyledonous and cereal plants. As a semi-aquatic species partly cultivated in lowland, rice is increasingly exposed to salt contaminated water, urging the need to breed and disseminate more salt tolerant varieties. The physiological responses of rice to salt have been extensively analyzed and reviewed, based on the study of a wide variety of sensitive and tolerant cultivars and wild relatives (Ponce *et al.*, 2021, van Zelm *et al.*, 2020).

Salt uptake and sensing by plant roots triggers rapid osmotic stress due to a reduction in water potential, followed by a slower ionic stress phase due to sodium toxicity in tissues (Yang and Guo, 2018). Early salt-induced responses include phospholipid signaling at the plasma membrane, initiation of specific calcium waves decoded by calcium-binding proteins and kinases followed by sodium channels activation like NHX7 involved in export of Na<sup>+</sup> out of the cell (van Zelm *et al.*, 2020). Salt stress rapidly induces reactive oxygen species (ROS) in the apoplast through the activation of respiratory burst oxidase homologs (Rbohs) and ROS act together with Ca<sup>2+</sup> signaling to affect cellular pH and ion homeostasis (Hasanuzzaman *et al.*, 2021). Ion distribution is orchestrated by multiple families of transporters whose members localize distinctly on the plasma membrane or endomembranes in cell specific patterns (Saddhe *et al.*, 2021) to exclude or sequester Na<sup>+</sup> ions. Continuous Na<sup>+</sup> uptake perturbs K<sup>+</sup> homeostasis, nutrient acquisition and compromises efficiency of cellular processes including photosynthesis, while inducing cell wall modifications (Liu *et al.*, 2021) and starch metabolism (Thalmann and Santelia, 2017).

Immediate salt responses further transduce into the complex reconfiguration of hormone metabolism and signaling programs (Yu *et al.*, 2020). Abscisic acid (ABA) is the dominant hormone that governs cellular and metabolic responses to drought or salt exposure (Sah *et al.*, 2016, Vishwakarma *et al.*, 2017). By promoting rapidly stomatal closure, ABA reduces evapotranspiration and controls overall water transport, in addition to modulating the



expression of arrays of genes involved in the adaptation response, including starch degrading enzymes (Thalmann and Santelia, 2017). Additionally, salt triggers a decrease in osmotic pressure and water loss, that is mostly compensated by the ABA-dependent accumulation of various osmolytes such as amino acids or sugar alcohols, and the induction of water deprivation responses.

More recent evidence indicates that several other plant hormones, acting in complex synergistic or antagonistic signaling cross-talks, impact salt responses and tolerance (Choudhary *et al.*, 2021, Yu *et al.*, 2020). Jasmonates (JAs) act as essential mediators of defense programs to biotic attacks (Heitz, 2021), but have also been associated with responses to various forms of abiotic stress (Kazan, 2015). In the case of salt tolerance, contrasting results and conclusions have been reported using different experimental setups or plant species, so that JA functions under salt stress are still debated (Delgado *et al.*, 2021, Riemann *et al.*, 2015). External treatments with JA were shown to attenuate salt-induced damage in some species like wheat (Qiu *et al.*, 2014) or barley (Walia *et al.*, 2007), but in *Arabidopsis*, salt triggers JA-mediated root growth inhibition (Valenzuela *et al.*, 2016) and external methyl-JA supply aggravates salt-triggered growth inhibition and senescence (Chen *et al.*, 2017). Furthermore, in tomato, a JA-deficient line exhibited enhanced oxidative stress and associated damage relative to wild-type (Abouelsaad and Renault, 2018). However, in rice, a growing body of evidence suggests that endogenous JA accumulation and signaling is detrimental to salt tolerance, at least at the seedling stage. Salt-induced inhibition of rice seminal root growth is mediated by ethylene-jasmonate interaction (Zou *et al.*, 2021). JA-deficient rice mutants *cpm2* and *hebiba* displayed less Na<sup>+</sup> accumulation and increased ROS-scavenging activity in shoots, correlated with attenuated damage upon salt exposure (Hazman *et al.*, 2015). Genes encoding catabolic enzymes acting on jasmonoyl-isoleucine (JA-Ile), the bioactive jasmonate hormone, have been identified in rice and are upregulated by salinity (Hazman *et al.*, 2019). Interestingly, a rice activation-tagging line overexpressing CYP94C2b, a cytochrome P450 oxidizing JA-Ile, displays enhanced survival rate under salt conditions (Kurotani *et al.*, 2015a). In addition, upon investigating a collection of extant rice accessions with various sensitivities, high salt-tolerance was found correlated with elevated expression of this gene (Kurotani *et al.*, 2015b). Among the known physiological and molecular responses of rice to salt, very few have so far been linked to JA signaling. Rice Salt Sensitive 3 (RSS3) is a nuclear factor that interacts with JAZ repressors to modulate the expression of JA-responsive genes and root cell elongation during adaptation to salinity (Toda *et al.*, 2013). Suppression or overexpression of JAZ9



antagonistically affects ion uptake with correlative impact on the expression of some ion transporter genes (Wu *et al.*, 2015). Together, these data suggest that reduced JA-Ile accumulation and/or signaling ameliorates the capacity of rice to withstand salinity.

Multiple transcriptome comparisons between sensitive and tolerant rice varieties have been reported (Formentin *et al.*, 2018, Kawasaki *et al.*, 2001, Li *et al.*, 2020, Mirdar Mansuri *et al.*, 2019, Razzaque *et al.*, 2017), but the peculiar biological processes and molecular targets regulated by JA signaling upon salt stress were not genetically addressed and remain largely unknown. In the present study, we compared the phenotypic, ionic, transcriptomic and several physiological characteristics of the Kitaake variety using the wild-type (WT) and a JA-deficient mutant interrupted in *ALLENE OXIDE CYCLASE* (*aoc*), an essential JA biosynthetic gene (Nguyen *et al.*, 2020). Extensive genotype comparison of transcriptomes in roots and shoot allow to pinpoint particular biological processes that are under JA regulation. We establish that absence of JAs confers an apparent better salt tolerance phenotype in seedlings, based on a optimized regulation of Na<sup>+</sup> distribution, and a delay in onset of senescence. However, JA deficiency substantially reduces the ABA content and water deprivation responses in leaf, resulting in impaired water management. Our study provides a rationale framework to understand the specific impacts of endogenous JA signaling on rice responses to salt stress.

## 2. MATERIALS AND METHODS

### 2.1 Plant culture and treatments

*Oryza sativa* L. ssp. japonica cv. Kitaake was used as WT and *aoc* as jasmonate deficient mutant (Nguyen *et al.*, 2020). Jasmonate deficiency leading to male sterility, *aoc* homozygous seedlings were isolated from the progeny of AOC/*aoc* plants. For salt stress experiments, caryopses of a segregating population were first preciously rinsed, placed on Petri dishes containing water imbibed Whatman paper, then placed for 4 days at 28°C in complete darkness for germination. Skotomorphogenic development in JA-deficient mutants leads to very long mesocotyl allowing the isolation of the *aoc* homozygous mutants. WT and *aoc* seedlings were then transferred to a floating styrofoam for hydroponic culture (MS solution: 358 mg L<sup>-1</sup> basal MS buffered with MES 42 mg L<sup>-1</sup>, pH 5.8) and incubated under continuous light of ~125 μmol m<sup>-2</sup> s<sup>-1</sup> at 28°C with 60% relative humidity. After 11 days growth, the MS solution was replaced



by a saline solution (MS solution containing 100 mM NaCl) for the salt treatment and a new MS solution for the mock treatment.

For MeJA treatment, WT rice seeds were dehusked and surface-sterilized through successive baths in 70% ethanol (1 min), distilled water (1 min) and in a sodium hypochlorite solution containing ~3 % active chlorine (20 min) followed by 4 washing steps with distilled water under sterile conditions. Seeds were then sown in magenta boxes containing 0.4% phytoagar medium in MS as above and cultivated under same conditions as for the salt experiment. After 7 days, a cotton wick with 20  $\mu$ L of pure MeJA was placed in each magenta box. All samples analyzed are constituted of a pool of tissues from three plants.

## **2.2 Stomatal conductance and relative water content (RWC)**

For stomatal conductance measurements, plants were raised in a hydroponic system as described above until the 5<sup>th</sup> leaves were fully expanded. Leaf stomatal conductance to water vapor (gsw) was measured with a LI-6800 portable photosynthesis system (LI-COR, Lincoln, NE) on the 5<sup>th</sup> leaf. Measurements were taken in an alternating manner from WT, mutant, control and stressed plants, respectively, from 1-7 h after day start (12 h days) to avoid bias imposed by the diurnal rhythm.

For RWC determination, leaf sheaths were collected from plants and immediately weighed to determine their fresh weight (FW). After 4 h hydration in plastic bags containing distilled water, the leaves were weighed again to measure the turgescent weight (TW). Then, leaves were dried for 24 h at 60° C and their dry weight (DW) was determined. RWC was calculated based on the following formula:  $RWC (\%) = [(FW-DW) / (TW-DW)] \times 100$  described by Barr and Weatherley (Barrs and Weatherley, 1962).

## **2.3 Electrolyte leakage**

Leaf blades were harvested and quickly rinsed in distilled water to remove ions on the leaf surface. Leaves were then cut into small pieces (1-2 cm) and floated onto 15 ml distilled water in 50 mL tube. After 1 h gentle shaking at room temperature, water electrical conductivity of solution was determined to estimate ion leakage. Samples were then boiled for 30 min before cooling for 1 h to room temperature. Solution conductivity was re-measured to estimate the total released ions. Percentage of released ions from dead cells was calculated using the following formula:  $[\text{conductivity at T0} / \text{conductivity of boiled samples}] \times 100$ .



## 2.4 Ion content measurement

Samples were ground frozen before being dried for 48 h at 60°C. Samples were digested using 0.5 mL ultrapure water, 2 mL HNO<sub>3</sub> (65% v/v, subboiled) and 0.5 mL H<sub>2</sub>O<sub>2</sub> (30% v/v, p.a.) in closed digestion tubes (Gerhardt, UK) in a heating block (DigiPrep jr, S-prep) system at 110°C for 3 h. Samples were evaporated to near dryness and after cooling final volume of each sample was adjusted to 20 mL with 1% v/v HNO<sub>3</sub> (subboiled). To check for the quality, we included blank samples and different reference materials (NIST 1573a (Tomato leaves), NCS ZC' 73013 (Spinach), Spruce needles (ring test) into the digestion procedure. Potassium and sodium content in the digest were measured by inductively coupled plasma optical emission spectrometry (ICP-OES, radial mode, iCap 7000, Thermo Fisher) in the Laboratory for Environmental and Raw Materials Analysis (LERA) at KIT. The accuracy of the reference material was in a good range with  $\pm 5.9\%$  (K) and  $\pm 7.1\%$  (Na) for the NIST 1573a,  $\pm 3.2\%$  (K) and  $\pm 3.52\%$  (Na) for the NCS ZC' 73013 and  $\pm 8.7\%$  (K) for the spruce needles.

## 2.5 Chlorophyll quantification

Frozen leaf samples were ground with glass beads (10 s, 5500 rpm, Precellys tissue homogenizer, Bertin Instruments, France) then homogenized with 80% cold acetone to extract chlorophylls (2 x 30 s, 5500 rpm). After sedimentation of cell debris by centrifugation, supernatant absorbance at 647 and 663 nm were measured to calculate the chlorophylls content based on the equations described in Porra *et al.* (1989).

## 2.6 RNA extraction and gene expression analysis

Frozen roots were ground manually in a mortar and total RNA was isolated using RNeasy Plant Mini kit (Qiagen). Leaf samples were ground using the glass-bead homogenizer before RNA isolation using Trizol Reagent according to manufacturer instructions. For the purpose of RNAseq, total RNA integrity was controlled after DNase treatment using a Bioanalyzer 2100 system with the RNA 6000 Nano Chip (Agilent Technologies, Santa Clara, USA). RNA with RNA integrity Number (RIN) value above 6.2 were used to construct cDNA libraries. Library construction and sequencing was performed at Novogene Europe (Cambridge, UK) on an Illumina platform (paired-end reads, 150 nucleotides). After exclusion of low quality reads and



reads with adaptors, clean reads were mapped to the reference genome Os-Nipponbare-Reference-IRGSP-1.0 using HISAT2. The resulting read counts were processed through the DIANE pipeline (Cassan *et al.*, 2021) for global normalization (EdgeR package), filtering of very low expressed genes (< 480 total read counts) and differential expression analysis (DeSeq2 R package) for which only genes with an absolute log<sub>2</sub> Fold Change (log<sub>2</sub>FC) ≥ 1 and an FDR < 0.05 were considered as DEGs. GO enrichment analysis was performed with the PANTHER classification system (geneontology.org; (Mi *et al.*, 2019) and focused on biological processes enriched with an FDR < 0.01.

For RT-qPCR analysis, cDNA was synthesized with Superscript IV Reverse Transcriptase (Thermofisher) using 2 µg of RNA. qPCR was performed using 20 ng of cDNA on a LightCycler 480 II instrument (Roche Applied Science, Penzberg, Germany) as described in Berr *et al.* (2010). The expression levels of the different targets were normalized against the expression level of the reference genes *UBQ5* (Os01g0328400) and *UBQ10* (Os02g0161900). The sequences of all primers used are listed in supplemental Table S4.

## 2.7 Hydrogen peroxide staining

3,3'-diaminobenzidine (DAB) staining was performed as described by (Daudi and O'Brien, 2012). Leaves of 5 days salt- and mock-treated rice seedling were collected, submerged in the DAB solution (1 mg mL<sup>-1</sup> DAB, 10 mM Na<sub>2</sub>PO<sub>4</sub>, 0.05% Tween). Since DAB is light sensitive, the preparation was covered with aluminum foil and incubated 4-5 h at room temperature under constant shaking (100 rpm). Leaves were then transferred to a clearing solution (ethanol/acetic acid/glycerol 3/1/1) and boiled for 20 min to bleach out the chlorophyll and reveal the H<sub>2</sub>O<sub>2</sub> staining.

## 2.8 Hormone profiling

Jasmonate/ABA profiling was performed as described in Marquis *et al.* (2022)

## 2.9 Statistical Analysis

All statistical analysis was performed on Rstudio. Comparisons of sample means were performed by one-way analysis of variance (P < 0.05) then Tukey's HSD multiple comparisons



tests. Significant differences of means were determined and represented using these following significant codes: “\*”:  $P < 0.05$ ; “\*\*”:  $P < 0.01$  and “\*\*\*”:  $P < 0.001$ ).

### 3 RESULTS

#### 3.1 Jasmonate deficient *aoc* mutant displays reduced symptoms upon salt stress

The Kitaake variety of rice was chosen for its short life cycle and the availability of a mutant line obtained by CrisprCas9. This line bears a disruption of the single copy *ALLENE OXIDE CYCLASE* (*AOC*) gene, encoding an essential activity for jasmonate biosynthesis (Nguyen *et al.*, 2020). Due to nearly full sterility, homozygous *aoc* plants were selected from a segregating population based on skotomorphogenic development after 4 days germination in the dark (Riemann, 2020), and then transferred for hydroponic cultivation for 7 days before exposure of roots to control or salt-containing solution. Salt exposure resulted in shoot growth inhibition as expected in both genotypes (Figure S1a), but reduction of seminal root length observed in WT was absent in *aoc* (Figure S1b), in accordance with previous results (Zou *et al.*, 2021). Among different concentrations of NaCl tested, 100 mM salt resulted in a differential tolerance phenotype visible from 4 days after onset of stress, and that was reminiscent of the observations of Hazman *et al.* (Hazman *et al.*, 2015) in the Nihonmasari cultivar. In WT Kitaake plants, the second (2<sup>nd</sup>) leaf first displayed severe symptoms of browning and drying starting from the leaf tip, whereas *aoc* 2<sup>nd</sup> leaf remained essentially symptom-free (Figure 1a). After longer times of incubation, the damage eventually spread to leaf 3 or even 4, while maintaining the genotype differential phenotype. Electrolyte leakage was measured as a readout of tissue damage and was found reduced in *aoc* leaves 2 and 3 relative to their WT counterparts (Figure 1b), confirming weaker disruption of tissue integrity in *aoc*.

#### 3.2 Salt stress triggers jasmonate metabolism with distinct patterns in rice roots and shoots

To investigate the time-resolved activation of jasmonate metabolism and signaling in WT plants, we collected separately root and 2<sup>nd</sup> leaf samples in a kinetic salt stress experiment, and submitted tissue extracts to quantitative jasmonate profiling by LC-MS/MS. Roots exhibited a rapid drop in their content in the JA precursor oxo-phytodienoic acid (OPDA) in response to salt, but JA levels remained stable throughout the experiment (Figure 2a). JA-Ile, the active



hormonal compound, was only occasionally detected (at very low levels in some replicates) in the early time points, whereas more significant increases were recorded at 3 and 5 days of stress. The more stable JA-Ile catabolite 12COOH-JA-Ile (Heitz *et al.*, 2012) was overaccumulated from 6 h and later on, indicating elevated metabolic flux through the JA-Ile pathway in salt-responding roots. In the second leaf, OPDA levels were low under control conditions and increased in a biphasic manner with an early peak between 1 and 6 h and a later one at 3-5 days post-salt exposure (Figure 2b), when visible tissue damage occurs. JA, JA-Ile and 12COOH-JA-Ile essentially followed similar dynamic trends than OPDA upon time, with 12COOH-JA-Ile being the highest accumulated compound. These results indicate the activation of complex jasmonate metabolism in rice seedlings in response to salt stress, with organ-specific temporal patterns and individual compound abundances in roots and in 2<sup>nd</sup> leaf.

### 3.3 Comparative analysis of differential transcriptome in WT and JA-deficient seedlings upon salt stress

To generate a global overview of the influence of jasmonate signaling on salt-triggered processes, we undertook a comparative transcriptome analysis in both roots and 2<sup>nd</sup> leaf of WT and *aoc* plants, in a kinetic study collecting samples at 0, 1 h, 6 h and 3 d after salt exposure. RNAseq was conducted on 3 independent biological replicates, and the distribution of samples in a two-dimensional Principal Component Analysis (PCA) was established. Root and shoot samples were largely separated, illustrating their unique transcriptomes (Figure S2a). When datasets from each plant organ were processed separately, additional time dispersions were visible. In roots, 1 h and 6 h time points were well separated from 0 h and 72 h (Figure S2b), whereas in leaf, 1 h samples remained close to 0 h (Figure S2c). After normalizing the full dataset, we extracted from WT data the expression patterns of genes involved in JA metabolism and signaling (Table S1) relative to 0 h. This analysis revealed early upregulation of several genes at 1 and 6 h in roots such as those encoding JA-Ile catabolic CYP94 enzymes (Hazman *et al.*, 2019) or JAZ proteins, and a biphasic induction in leaf at 1 h and 72 h (Figure 3a). These transcriptional behaviors closely mirror the distinct patterns of hormone/catabolite variations (Figure 2) and further illustrate that salt stress activates distinct JA signaling dynamics in below-ground and aerial parts of the plant.

We next filtered differentially expressed genes (DEGs) within each organ, with respect to time and genotype comparisons, using a log<sub>2</sub> Fold Change (logFC) of  $-1 < \log_2\text{FC} < 1$  and a false



discovery rate (FDR) < 0.05. Before salt stress application, a significant number of DEGs (179 in roots, 964 in 2<sup>nd</sup> leaf) were revealed between *aoc* and WT (Figure 3b, 0 h). In time comparisons relative to their respective 0 h (Figure 3c), DEGs were most abundant at early (1 h and 6 h) time points after salt exposure in roots, whereas their rise in leaf occurred later at 6 h and 72 h (Figure 3c). In direct genotype comparisons (Figure 3b), except at 0 h, expression of a majority of DEGs were found reduced (labelled as down) in *aoc* mutant relative to WT at all time points. This suggests that jasmonate signaling contributes significantly to the massive gene expression reprogramming under salt stress conditions.

### 3.3.1 Transcription factor gene dynamics and JA-dependence

To globally estimate the extent of transcriptional changes that are under JA control, we set out to determine the dynamics of transcription factor (*TFs*) gene expression upon salt response, in particular with regards to their differential expression in both genotypes. Expression data were analyzed in time comparisons ( $-1 < \log FC < 1$ ; FDR < 0.05), and organized as UpSet diagrams (Lex *et al.*, 2014), that allow to intersect distinct expression patterns at one or several time points and visualize common or diverging behaviors in WT or *aoc*. In roots, both genotypes show about the same number of deregulated TFs at all time points after salt exposure, with the largest set of TF genes upregulated at 1 h, and their number then declined (Figure 4a left panel). Few TFs were specifically upregulated in *aoc* or WT (21 and 19 at 1 and 6 h in WT respectively) compared to the many (71 at 1 h, 23 at 6 h and 39 at 1 and 6 h) found similarly affected by salt in both genotypes. For salt-downregulated TFs in roots, genotype-specific behaviors were more common, mostly at 1 h and 72 h, indicating a stronger influence of JA signaling. In 2<sup>nd</sup> leaf, WT shows much more up-regulated TF genes at 1 h and 72 h than *aoc* but, in contrast, less down-regulated TF genes at all time points after salt exposure. These differences reflect particularly in large sets of TF genes specifically responsive in WT at 1 h (35 TFs) and 72 h (56 TFs) after salt exposure. The analysis indicates a significant influence of JA signaling on regulators of the leaf salt response, with mostly positive and few negative impacts of this hormone on TF gene expression. Finally, we crossed the lists of genotype-differential (*aoc* vs WT) TF genes in root with those in shoot (Figure S3). This highlighted the low proportion of shared TFs, suggesting that distinct JA-controlled regulators are driving transcriptional changes in below and above-ground parts of rice plants under salt.



As a case study, we next extracted the TF genes that are exclusively deregulated on one hand at 1 h and 6 h in WT root, and on the other hand at 1 h and 72 h in leaf, which are the materials where JA accumulation (Figure 2) and signaling (Figure 3a) was demonstrated. These genes are unresponsive in *aoc* and therefore likely to be activated in a JA-dependent manner and control JA-mediated processes. By doing so, we identified genes -mostly in leaf- that were previously associated to various extents with drought, dehydration, ABA, or abiotic stress responses but whose JA-dependence was largely unknown (Table 1). In addition, the filtering retrieved TF genes of the zinc finger, MYB, AP2, bHLH or WRKY families that were not previously linked to JA-dependent salt responses. This finding suggests a significant contribution of JA signaling to the water deprivation component of salt stress. Additional TF expression intersections can be filtered from Table S2 to investigate specific dynamic behaviors.

### **3.3.2 Gene ontology analysis reveals biological processes impacted by jasmonate signaling upon salt stress**

To sort out the biological processes affected with regard to organ, time and genotype, general DEG lists were submitted to gene ontology (GO) analysis, and GO terms were displayed as kinetic heatmaps. Two types of comparisons were utilized to extract biological information: on the one hand, were plotted time comparisons with enrichment of terms in salt-exposed samples relative to 0 h of respective genotype (Figure 5), and on the other hand genotype comparisons where *aoc* and WT enrichments were directly compared at each time point (Figure S4). Major known JA-dependent responses including genes involved in defense to biotic stress or wounding, as well as many genes encoding JAZ repressors were enriched throughout the whole kinetic in WT leaf, meaning their loss in *aoc* (Figure S4c right panel), whereas such a differential pattern was only recorded at 1 h and 6 h in roots (Figure S4a). Before stress (0 h), specific behaviors emerged for oxidative stress- and cell wall-related genes. For example, 5 class III peroxidase genes were less expressed in *aoc* roots (Figure S4a), whereas in *aoc* leaf, nearly 20 peroxidase (Figure S5b) and 5 laccase genes were stronger expressed at 0 h, along with genes involved in secondary cell wall biogenesis, encoding cellulose synthases, expansins, pectin-methylesterases or hybrid prolin-rich proteins (HyPRPs) (for individual genes, see Table S3). This illustrates a significant and contrasted impact of JA signaling on the transcriptome under optimal growth conditions.



After exposure of roots to salt, numerous changes in GO term enrichment were recorded relative to non-stressed controls. Many of them had similar trends in the two genotypes, such as protein folding responses or response to heat that were shortly down at 1 h (Figure 5a bottom panel). Unexpectedly, several terms related to nitrate homeostasis, including *NRT* transporters and nitrate response genes, were downregulated at 72 h in *aoc* roots only. Among up-regulated terms, different terms related to ABA biosynthesis/responses, or water deprivation/osmotic responses showed various enrichment patterns: some transiently up in *aoc* at 1 h, related terms enriched only later in WT (Figure 5a, Table S3) (*see paragraph below*). Consistently, a number of known JA-regulated responses to biotic stress were enriched in WT (Figure S4a right panel). More surprisingly, several photosynthesis-related terms were found enriched in WT roots at 72 h only. This may result from the hydroponic culture that favors greening of roots (Figure S4b); however, expression magnitude of these genes remained marginal in roots compared to shoots. Conversely, other terms were enriched at 72 h in *aoc* roots, such as some defense-related genes including several chitinases (also in ‘cell wall catabolic process’ term), *SUCROSE SYNTHASE* 7, and *SWEET* sugar transporters. These may represent JA-repressed components of carbohydrate metabolism and transport in roots.

The transcriptional landscape in 2<sup>nd</sup> leaf appeared largely different. Few (147) genes were downregulated by salt relative to 0 h at 1 h in WT, in contrast to *aoc* (765) (Figure 3c). In *aoc*, genes associated with lignin polymerization (7 laccases) dropped transiently. As well, most GO terms linked to cell wall biogenesis and oxidant detoxication, response to oxidative stress (mostly peroxidases) that were found enriched in *aoc* leaf at 0 h (Figure S4c left panel) were downregulated from 1 h to 72 h (Figure 5b bottom panel; Figure S5b). In addition, numerous terms related to water deprivation and ABA response were enriched in the up-response at 1 h and 72 h in WT but barely in *aoc*. These comprised for example genes encoding dehydrins, trehalose biosynthesis and cell wall biogenesis functions (Figure 4b right panel top, *see paragraph below*) and suggests that several processes are absent in *aoc* leaf at early time points of the salt response. In the genotype comparison, an enrichment in photosynthesis terms (‘light harvesting, pigment biosynthesis process’) in *aoc* is prominent (Figure S4c), indicating that the mutant may be prone to better maintain photosynthetic capacity under salt stress. At 6 h salt exposure, the response amplified in leaf, with a bulky group of terms that is shared between genotypes but with extended expression in *aoc*, and which relates to RNA processes, such as exosome complex components, mRNA surveillance and processing, and ribosome assembly (Figure 5b). This could be interpreted as a recovery/compensatory response of the leaf to the



initial rapid osmotic stress. Consistent with higher expression of photosynthesis components at 1 h, *aoc* leaves exhibited an enrichment in genes related to starch synthesis, recorded at 72 h (Figure 5b, top panel ‘glycogen biosynthetic process’), which is reflective of a better energetic status of *aoc* leaf. A persistent anabolic activity is also illustrated by enrichment of primary cellular functions in *aoc* at 72 h such as protein translation or amino acid biosynthetic processes. This was accompanied by the upregulation of a large set of glutathione S-transferase genes at 72 h (Table S3).

The global analysis therefore disclosed a significant impact of JA signaling, on root but more substantially on leaf transcriptome. Specific processes are altered in non-stressed conditions, but differential features were more prevalent upon salt stress, where JA deficiency seems to impair full induction of leaf ABA responses and oxidative stress related genes, and conversely allows for sustained maintenance of photosynthetic and carbohydrate storage components.

### **3.4 JA signaling is required in leaves but not in roots for ABA biosynthesis and water deprivation management under salt stress**

Given their genotype-specific GO term enrichment and importance in salt tolerance, ABA metabolism and water deficiency responses were further investigated. Genes encoding ABA biosynthetic or catabolic activities were examined, and their expression was found similarly salt-induced in roots of both genotypes (Figure 6a; Table S3). In contrast, their bi-phasic expression recorded at 1 h and 72 h in WT leaves, in particular for the induction of the rate-limiting *NCED* genes in ABA biosynthesis, was lost in *aoc*. Consistently, ABA contents in both organs supported these distinct expression patterns. In roots, ABA levels peaked similarly at 1 h in WT and *aoc* and declined thereafter, whereas in leaf, ABA build-up was weaker in *aoc* compared to WT at 3 time points (Figure 6b). Concerning water deprivation response genes that are largely under ABA control, their root response remained essentially unaffected by JA deficiency, but in leaf, two groups of genes with distinct behaviors were revealed: the largest group including a number of signaling genes encoding PYL receptors, TFs or a MAP kinase and behaved similarly in *aoc* and WT (Figure 6c). This was in contrast with a smaller group of genes including *RAB* and *dehydrin* genes that were co-induced with JA pulses at 1 h and 72 h in WT, but were downregulated or unresponsive in *aoc*. Of note, expression of *OSCA1.1* (Os01g0534900), encoding a hyperosmolality-gated calcium channel (Zhai *et al.*, 2021) was slightly reduced in both *aoc* organs (Table S3). Following our observation of accelerated rolling of *aoc* detached leaf material upon symptom imaging, we determined that stomatal conductance



to water (gsw) dropped dramatically upon salt stress, reflecting stomatal closure, but significantly less in *aoc* (Figure 6d). Consistently, relative water content (RWC) was significantly reduced in *aoc* compared to WT upon salt stress (Figure 6d). Altogether, our results indicate that while the ABA transcriptional response remains largely functional in roots, in leaves, disrupted JA pathway prevents the full activation of ABA biosynthesis and optimal induction of osmotic stress/water deprivation responses, which in turn impinges on proper water management.

### 3.5 JA signaling contributes to ion homeostasis and root-to-shoot sodium translocation

Sodium uptake by roots upon salt exposure imposes ionic stress throughout the plant that negatively affects cellular processes (Yang and Guo, 2018). Ion homeostasis that is maintained by various ion transporters is perturbed by Na<sup>+</sup> influx, and adaptation mechanisms are required, for example, to sequester Na<sup>+</sup> in vacuoles or exclude it from cells to lower cytoplasmic concentrations (Saddhe *et al.*, 2021). Very little is known to which extent JA signaling is involved in modulating ion transporter gene expression, or how it impacts long-distance Na<sup>+</sup> transport. *OsJAZ9* misexpression was reported to modulate a few transporters (Wu *et al.*, 2015), but no systematic analysis has been conducted so far. Individual ion transporters within multigene families have particular expression patterns and may encode distinct specificities, making it difficult to infer profiles from general GO analysis. Hence we undertook a more specific examination of JA impact on ion transporter expression by inspecting the profiles of about 70 rice genes (Table S1) that encode confirmed or putative Na<sup>+</sup> or K<sup>+</sup> transporters. Genes for which expression was differential in at least one time comparison (Table S3) in either genotype ( $-1 < \log_{2}FC < 1$ , FDR < 0.05) were compiled in a heatmap. This retrieved 26 and 41 transporter genes from root and leaf analysis respectively (Figure S6). Contrasted expression patterns were revealed, with both down- and up-regulation of various members; most of these perturbations were comparable in parallel time-analysis of *aoc* and WT in roots and shoot, indicating that these regulations were largely JA-independent. When expression was compared on a genotype basis at each time point, more specific features emerged: in 2<sup>nd</sup> leaf, most differentially expressed transporter genes were downregulated in *aoc*, including several members of the cation/proton exchanger family (CHX) of which some were associated positively or negatively to salt tolerance (Jia *et al.*, 2021). In roots, two transporter genes were strongly differential: *HAK4* and *HAK16* were found significantly more expressed at 72 h in *aoc* roots relative to WT (Figure 7a and Figure S8b). *HAK16* is a plasma membrane-localized



transporter involved in K<sup>+</sup> uptake and translocation to shoots (Feng *et al.*, 2019). HAK16 belongs to cluster I of HAK transporters that are involved in K<sup>+</sup> uptake and translocation to shoots (Feng *et al.*, 2019, Véry *et al.*, 2014). HAK4 belongs to the cluster IV which groups HAK transporters closely related to PpHAK13, a Na<sup>+</sup> permease identified in *Physcomitrium patens* (Véry *et al.*, 2014). Specificity of the rice HAK4 for Na<sup>+</sup> rather than K<sup>+</sup> transport has been recently established in a report of ZmHAK4 that was characterized in maize as conferring natural variation of shoot salt tolerance owing to its role in Na<sup>+</sup> exclusion from xylem sap (Zhang *et al.*, 2019). In the same study, the rice ortholog (*OsHAK4*) was found similarly expressed in the root stele and exhibited comparable ion transport properties. Consistent with its elevated expression in JA-deficient *aoc* roots, *OsHAK4* expression in WT was progressively repressed by external JA treatment experiment (Figure 7b).

To examine how such differential expression patterns of transporter genes relate to actual ion accumulation, we determined Na<sup>+</sup> and K<sup>+</sup> contents in roots and leaves before and 5 days after salt exposure. In our conditions, K<sup>+</sup> content was not affected by JA deficiency (Figure 7c). In roots, salt exposure reduced K<sup>+</sup> content by half with no JA-dependence, but salt had essentially no influence on K<sup>+</sup> content in 2<sup>nd</sup> and 3<sup>rd</sup> leaves. Na<sup>+</sup> content increased significantly to higher levels in *aoc* compared to WT roots upon stress. In contrast, Na<sup>+</sup> accumulation was reduced by 44% in 2<sup>nd</sup> *aoc* leaf relative to WT whereas no difference was recorded in 3<sup>rd</sup> leaf. This indicates that higher *HAK4* expression levels correlate with enhanced Na<sup>+</sup> retention in *aoc* roots and lower Na<sup>+</sup> translocation to 2<sup>nd</sup> leaf, a relationship that could sustain the better salt tolerance of *aoc* leaf.

### 3.6 JA signaling controls discrete ROS detoxifying genes

Salt stress comes along with oxidative stress whose degree of management is an important parameter affecting tissue survival (Hasanuzzaman *et al.*, 2021, Liu *et al.*, 2020). We previously analyzed the activity of the enzymatic ROS in *cpm2* and *hebiba* mutant lines in leaves at 72 h post salt exposure and found that total glutathione S-transferase (GST), peroxidase (POD) and superoxide dismutase (SOD) activities were elevated in JA-deficient leaves compared to WT (Hazman *et al.*, 2015). Similar to the Nihonmasari cultivar used in that study, here DAB staining of ROS in Kitaake 2<sup>nd</sup> leaf visualized stronger signal in WT relative to *aoc* in response to salt, confirming reduced H<sub>2</sub>O<sub>2</sub> accumulation in absence of JAs (Figure 8a). Concerning transcriptome data, we screened the behavior of nearly 200 genes (Table S1) encoding ROS-



scavenging or -consuming activities, including ascorbate (APX) and class III peroxidases, catalases, GST, POD, RBOH and SOD. A majority of salt-triggered changes were similar in both genotypes, and are thus largely JA-independent (Figure S7a). Several *GST* genes appeared however less stimulated, or downregulated by salt in *aoc*, indicating a partial JA-dependence. The genotype comparison highlighted several *GST* genes that were more expressed in *aoc* leaves at 0 h (along with many POD genes, see Figure S5b), possibly protecting tissues even in non-salty conditions, but only *GSTU16* remained upregulated at 72 h in *aoc* (Figure 8b). In addition, this comparison disclosed the sustained expression in *aoc* leaf of three *SOD* genes: the Cu/Zn-dependent *SOD2* at 1 h, and *FSD1.1* and *FSD1.2*, encoding Fe-dependent chloroplastic SODs. Normalized counts of these candidate targets were plotted in Figure S8a and illustrate lower expression in WT. FSD activity may sustain stronger superoxide dismutation into less toxic hydrogen peroxide in sodium-challenged chloroplasts and alleviate salt-induced damage. Consistently, exogenous JA treatment repressed *FSD* expression in WT plants, confirming their negative regulation by JA signaling (Figure 8c). Altogether, JA deficiency better maintains or derepresses specific genes that could underlie the amelioration of distinct ROS scavenging activities.

### 3.7 JA deficiency delays salt-induced senescence and chlorophyll degradation

Salt intoxication along with oxidative stress are known to result in accelerated leaf senescence (Figure 1) involving mainly ABA-mediated responses, but the specific contribution of JA signaling is less characterized (Lee and Masclaux-Daubresse, 2021). We therefore examined 27 rice genes (Table S1), annotated as Senescence Associated (SAG), for their transcriptional behavior in leaf. Many SAGs were salt-induced in WT, particularly at 72 h (Figure S7b), including those encoding known transcription factors acting as positive regulators of senescence, such as *ERF101* (Lim *et al.*, 2020) or *NAP* (Liang *et al.*, 2014). Both time- (Figure S7b) and genotype-comparisons (Figure 9a) showed that their expression was lower in *aoc* leaf, in terms of intensity or timeframe, along with reduced expression of senescence execution genes such as *Chloroplast vesiculation CV* (Sade *et al.*, 2018), chlorophyll degrading genes including *StayGreen (SGR)* or *NYC1*, consistent with the phenotypically delayed senescence in *aoc*. Furthermore, the SAGs *OsI43* and *NAP* were confirmed to be JA-inducible upon exogenous treatment (Figure 9b). The impaired induction of genes promoting chlorophyll degradation is consistent with the stress-resilient expression of chlorophyll and other pigment



biosynthesis genes in *aoc* leaf when those decline in WT (Figure S4c). Consistently, *VTE3*, encoding a methyltransferase (Os07g0179300) in the biosynthesis of the chloroplastic antioxidant  $\alpha$ -tocopherol (Muñoz and Munné-Bosch, 2019) was higher expressed in *aoc* leaf in control and early stages of the response (Table S3). Inhibition of senescence-associated catabolic processes in *aoc* leaves was supported by the stability of chlorophyll content under salt stress (Figure 9c). In contrast, WT damaged 2<sup>nd</sup> leaf reduced by 39% its chlorophyll content while content remained stable in 3<sup>rd</sup> leaves that were symptomless in this experiment. These differential expression data provide a molecular basis for a delayed salt-induced senescence in JA-deficient rice.

#### 4. DISCUSSION

Plant exposure to excessive salt affects a myriad of biological processes and triggers complex adaptive changes to maintain physiological functions. Responses to salt stress have been extensively addressed in numerous model and non-model plant species at the physiological, cellular and molecular levels, and a number of tolerance-associated genes have been identified (Arif *et al.*, 2020, Ponce *et al.*, 2021, van Zelm *et al.*, 2020, Yang and Guo, 2018). Central to adaptation responses, hormonal interactions orchestrate complex reconfigurations (Choudhary *et al.*, 2021, Yu *et al.*, 2020). Most hormonal pathways are perturbed upon plant exposure to salt, typically abscisic acid is increased and directs many beneficial responses, but negative effects on tolerance have also been reported as for cytokinins or ethylene (Yang *et al.*, 2015). Jasmonate positive impacts in adaptation to some abiotic stresses such as cold or drought are being consolidated (Kazan, 2015, Marquis *et al.*, 2022, Riemann *et al.*, 2015). In contrast, understanding JA functions in salt tolerance is still blurred by contradictory reports between exogenous JA application -which may ameliorate tolerance-, and genetic data in rice from either JA biosynthetic mutants (Hazman *et al.*, 2015) or high catabolic lines (Kurotani *et al.*, 2015a, Kurotani *et al.*, 2015b), which suggest detrimental impacts of JA on salt tolerance. To solve this paradox, a side-by-side kinetic comparison was undertaken between a recently-established mutant that is fully devoid of JAs (Nguyen *et al.*, 2020) and its wild-type in the rapidly-growing cultivar Kitaake. Our goal was less to exhaustively describe transcriptional changes triggered by salt, that are widely documented in rice (Formentin *et al.*, 2018, Kong *et al.*, 2019, Li *et al.*, 2020, Zhang *et al.*, 2022), than to map biological processes -and when possible individual genes- whose activity vary in presence or in absence of a functional JA biosynthetic pathway.



We analyzed simultaneously roots and first emerged leaves (2<sup>nd</sup> and 3<sup>rd</sup>) as salt is sensed first in roots and tissue damage was recorded primarily in leaf, and also because whole plant Na<sup>+</sup> management is critical to aerial organ tolerance. Under the conditions used, that impose a limited osmotic constraint before Na<sup>+</sup> toxicity builds-up, a clear differential phenotype was obtained with WT 2<sup>nd</sup> leaf undergoing extensive damage from day 4-5 while *aoc* remained essentially symptomless, a trend that later extends to new emerging leaves. These observations comfort a previous report in Nihonmasari cultivar (Hazman *et al.*, 2015) and demonstrate that interrupted JA biosynthesis mitigates damage in rice response to salt at the seedling stage. They further suggest that some JA-controlled processes translate into suboptimal resilience to salt.

To establish a comprehensive picture of jasmonate accumulation dynamics upon salt stress, detailed hormone profiling was performed in WT rice plants, revealing distinct patterns in each organ (Figure 2). In roots, early consumption of pre-existing precursor OPDA seemed to be at the basis of JA-Ile synthesis and catabolism with low amplitude. In 2<sup>nd</sup> leaf, all four analyzed compounds exhibited bi-phasic accumulation by 1 h and later by 3-5 days, the late increase being concomitant to leaf symptom appearance. The rapid pulses recorded here were frequently missed in previous studies. These hormonal patterns were consistently matched by JA pathway gene expression dynamics and together, the data highlight the organ-specific timeframes of activation of JA metabolism and signaling: within the first hours of salt exposure in roots, whereas the leaf response expresses as an immediate pulse by 1 h followed by a longer lasting activation starting by day 3. It is tempting to interpret that the early JAs accumulation may be due to the rapid osmotic stress component of salt exposure, and the second wave to consequences of the slower Na<sup>+</sup> accumulation in tissues.

Differential expression (DEGs) was mined for each organ in two dimensions: time-resolved comparisons allowed to assess dynamics relative to untreated controls, but such readouts are impacted by expression levels at 0 h which may vary for some genes between *aoc* and WT. Data were thus also compared directly between genotypes at each time point. Overall, DEGs number was highest at 1 and 6 h in roots and more delayed in leaf, reflecting long-distance spread of signaling and organ-specific responses. TF genes could be readily filtered for peculiar behaviors throughout the kinetic. For example, a number of TFs regulated only in WT were identified, and are thus JA-dependent; a few have previously been associated with drought or ABA responses, but others are of unknown function. In a global investigation, DEG lists were submitted to GO term enrichment analysis, of which only the most prominent outcomes can be



discussed here. The study should be taken as a resource that can be mined for many more processes than could be addressed presently. For example, many cell wall-related terms were perturbed by JA-deficiency in various ways before or after stress. The constitutive upregulation of expansins or HyPRPs in *aoc* leaf relates to two recent findings: ectopic overexpression of *EXP7* increases salt tolerance by promoting antioxidant activity, cell elongation and ion homeostasis (Jadamba *et al.*, 2020); as well, HyPRP06 regulates salt tolerance via apoplastic ROS homeostasis (Zhao *et al.*, 2022). By extension, the elevated expression of many class III peroxidases in *aoc* leaf may alter the redox status of the apoplast and facilitate cell wall integrity maintenance under salt (Liu *et al.*, 2021).

At least four major differential features emerged from the comparative transcriptome analysis, even though additional processes in the dataset deserve attention in the future:

1. The ABA pathway, whose activation is essential to the rapid response to abiotic stresses (Raghavendra *et al.*, 2010), was selectively impaired in JA-deficient *aoc* mutant. Global assessment indicated an enrichment in ABA-related GO terms in WT leaves, meaning their under-representation in *aoc*. Upon closer examination, a contrasted picture emerged: only a few ABA-induced targets, including the TF *ZFP36* controlling antioxidant defense (Zhang *et al.*, 2014) were depressed in *aoc* roots, consistent with their near-WT ABA content (Figure 6). In contrast, ABA biosynthetic gene expression and ABA hormone build-up were much lower in the early phase of the response in *aoc* leaf, correlated with a strongly reduced expression of some -but not all- targets such as several *RAB* or *DHN* genes. This impaired ABA response was reflected physiologically by an incomplete drop in stomatal conductance in *aoc* leaf in response to salt, resulting in a reduced water content due to excessive transpiration in these tissues. The importance of ABA-JA interactions under drought was recognized previously in Arabidopsis (de Ollas and Dodd, 2016). Our findings highlight a distinct hormone interaction in under- and above-ground organs: roots deploy a proper ABA response in absence of JA, while adaptation to water deprivation in rice leaves relies on a positive ABA-JA crosstalk, at least for a peculiar sub-branch of the response. This also coincides with the independent observation that JA signaling is required in rice to withstand osmotic stress (Tang *et al.*, 2020).

2. A second major aspect affecting salt tolerance is linked to variations in management of Na<sup>+</sup> that floods the successive cell layers. Global expression survey illustrated the very diverse expression changes of ion transporters, even within a given gene family. Probably various



subcellular, cellular, tissue and organ-specific ion transporters show distinct reactivities to the massive influx of Na<sup>+</sup>. Most of these dynamics, irrespective of their importance under normal or stress conditions, were found unaffected by the status of JA signaling (Figure S6). Because Na<sup>+</sup> management and tissue content are critical parameters for salt tolerance (Ganie *et al.*, 2021, Ponce *et al.*, 2021), and JA-deficient rice mutants were reported to accumulate less Na<sup>+</sup> in leaves (Hazman *et al.*, 2015), we sought to identify candidate ion transporter genes that were impacted by JA signaling and that could account for differential Na<sup>+</sup> homeostasis in *aoc*. By filtering the genotype comparison, a low number of *aoc* leaf-downregulated genes popped-up from the CHX and HAK families (Figure 7) and could be at the basis of distorted ion homeostasis. More specifically, *HAK4* and *HAK16* were salt-repressed in WT but not in *aoc* roots. This is in contrast to *HAK12*, *17* and *24* that were salt-induced, irrespective of the JA biosynthetic capacity (Figure S6). *HAK16* functions in K<sup>+</sup> uptake and translocation to shoots (Feng *et al.*, 2019), and its root derepression correlates with unaltered K<sup>+</sup> content in *aoc* leaf under salt conditions (Figure 7c). *HAK4* was only recently characterized as a root transporter in rice and in maize where it confers natural variation of salt tolerance. In both species, it is believed to exclude Na<sup>+</sup> from xylem sap (Zhang *et al.*, 2019). Here, its upregulation in rice *aoc* roots, indicative of a JA-repression in WT, is fully consistent with more Na<sup>+</sup> being retained in *aoc* roots and less being translocated to shoots (Figure 7c), possibly contributing to attenuate leaf damage. This result constitutes a rationale basis to investigate genetically the potentially unique function of OsHAK4 in the JA-dependent control of root-to-shoot Na<sup>+</sup> translocation.

3. ROS production and subsequent activation of detoxication systems are integral to the build-up of salt stress. JA deficiency resulted in genotype differential expression of a number of genes encoding ROS-metabolizing activities or affecting redox status. A large number of genes encoding apoplastic H<sub>2</sub>O<sub>2</sub>-consuming class III peroxidases were stronger expressed in non-stressed *aoc* leaf, which may contribute to lower resting ROS levels and better buffering of subsequent salt-induced ROS burst. In particular, a repression by JA signaling in WT of the Fe-dependent *FSD1.1* and *FSD1.2* was uncovered and point to a better superoxide ion scavenging in chloroplasts of *aoc* leaves (Figure 8). This reinforces chloroplasts as important sites for cell death initiation under salt stress in rice (Ambastha *et al.*, 2017).

4. More directly linked to the visual leaf damage phenotype are the processes related to senescence. While the developmental senescence-promoting activity of JAs along with other stress hormones including ABA and ethylene is well-described (Wojciechowska *et al.*, 2018),



the extent to which JA signaling activates salt-induced senescence pathways was largely unknown. Here, the combined analysis of SAG expression, leaf tissue integrity and chlorophyll content establishes that JA signaling is a major mediator for the execution of senescence processes under salt stress in rice. Suppressing JA biosynthesis in *aoc* impaired or delayed most of these programs, resulting in extended viability of vegetative tissue. This is in full accordance with the delayed salt-induced senescence observed in a rice line overexpressing a JA-Ile catabolic gene (Kurotani *et al.*, 2015a). Moreover, the partial impairment of ABA signaling in *aoc* leaves could also underlie delayed senescence.

In conclusion, the extensive transcriptome and physiological analysis performed in this study have disentangled some of the contradictory results reported as to negative or positive impact of JA signaling on salt tolerance (summarized in Figure 10). Salt concentrations and timing applied are important parameters as to the relative strengths and dynamics of osmotic and ionic components of the stress. While it is difficult to establish a precise timeline of JA-dependent events because many components occur simultaneously in a given organ, a common starting feature is the early (1 h) hormonal response that translates into distinct transcriptional changes in root and shoot. We demonstrate that JA is required for ABA to co-regulate positively responses limiting water loss and that JA signaling triggers several pathways leading later on to salt-triggered leaf senescence. These JA-stimulated biological processes are coordinated and converge to accelerate tissue damage when ionic toxicity culminates. Within cell wall-related perturbations, some JA-dependent upregulated pectin methyl esterases in WT could trigger a reported MeOH-JA cascade that promotes senescence (Fang *et al.*, 2016). Conversely in *aoc*, increased expression of *HAK4*, a transporter gene under negative JA regulation, correlates with higher Na<sup>+</sup> retention in roots, protecting leaves where less toxic Na<sup>+</sup> is accumulated, senescence machinery remains silent, along with increased ROS scavenging capacity in chloroplasts. These different physiological features are in accordance with similar traits recorded in a recent study with JA-defective maize seedlings (Ahmad *et al.*, 2019). The present transcriptome dataset needs to be further explored to decipher the deeper consequences of JA signaling onto responses to salt; as an example mineral nutrition would be an important target to follow throughout the plant's lifecycle. With such dual impacts, JA signaling cannot be associated strictly anymore to either salt sensitivity or tolerance.



## SUPPLEMENTAL DATA

**FIGURE S1.** Developmental phenotypes of rice wild-type (WT) and jasmonate-deficient (*aoc*) seedlings exposed to control or 100 mM NaCl (salt) solutions.

**FIGURE S2.** Principal component analysis (PCA) of RNAseq data distribution.

**FIGURE S3.** Overlap of deregulated transcription factor genes in shoots and roots

**FIGURE S4.** Gene ontology (GO) analysis of differentially expressed genes (DEGs).

**FIGURE S5.** Kinetic expression profile of rice class III peroxidase genes displayed as heatmaps in root (a) and 2<sup>nd</sup> leaf (b).

**FIGURE S6.** Kinetic expression profile of rice ion transporter genes displayed as heatmaps in root and 2<sup>nd</sup> leaf.

**FIGURE S7.** Kinetic expression profile of rice genes encoding ROS-scavenging or – consuming activities displayed as heatmaps in root and 2<sup>nd</sup> leaf of *aoc* and WT plants.

**FIGURE S8.** Kinetic expression profile of rice genes identified as probable targets of JA signaling upon salt stress.

**TABLE S1.** Lists of selected pathway genes that were screened for salt- and JA-regulated expression.

**TABLE S2.** Matrix of differential expression for genes encoding rice transcription factors.

**TABLE S3.** Global gene expression table in WT and *aoc* rice seedlings upon salt stress.

**TABLE S4.** Primers used for RT-qPCR experiments.

## ACKNOWLEDGMENTS



We thank L. Malherbe, C. Kotschenreuther, and J. Wagner for technical assistance, and A. Soriano for advices in early transcriptome analysis with DIANE pipeline. We are grateful to J. Zumsteg for technical help in LC-MS/MS analysis and A. Berr for access to conductimeter. We thank A.-A. Véry for helpful insight into ion transporter properties.

## **AUTHOR CONTRIBUTIONS**

TH, SN, MR and AC collectively designed the experiments. SN, THN, EE and TH performed most of the experiments. NP, FB and SS performed LI-COR measurements. VC and DP contributed to RNAseq data processing. TH, SN, AC and MR analyzed data. TH wrote the article with input of SN, MR and AC.

## **CONFLICT OF INTEREST**

The authors declare having no conflict of interest

## **FUNDING**

SN was supported by an international doctoral fellowship from the Investissements d'Avenir (IdEx) program from Université de Strasbourg. RNAseq experiments were funded by a grant from Bayer Foundation to SN. The study benefited mobility grants from CampusFrance, DAAD (Germany) mobility funding and a grant from the European Campus (Eucor) program.

## **DATA AVAILABILITY**

Data supporting the findings in this study are available within the paper and within its supplementary materials published online. The raw and normalized RNAseq data were submitted to the NCBI Gene Expression Omnibus repository under accession GSE206706.



## REFERENCES

- Abouelsaad I, Renault S.** 2018. Enhanced oxidative stress in the jasmonic acid-deficient tomato mutant *def-1* exposed to NaCl stress. *Journal of Plant Physiology* **226**, 136-44.
- Ahmad RM, Cheng C, Sheng J et al.** 2019. Interruption of Jasmonic Acid Biosynthesis Causes Differential Responses in the Roots and Shoots of Maize Seedlings against Salt Stress. *International Journal of Molecular Sciences* **20**, E6202.
- Ambastha V, Sopory SK, Tiwari BS, Tripathy BC.** 2017. Photo-modulation of programmed cell death in rice leaves triggered by salinity. *Apoptosis* **22**, 41-56.
- Arif Y, Singh P, Siddiqui H, Bajguz A, Hayat S.** 2020. Salinity induced physiological and biochemical changes in plants: An omic approach towards salt stress tolerance. *Plant Physiology and Biochemistry* **156**, 64-77.
- Barrs HD, Weatherley PE.** 1962. A Re-Examination of the Relative Turgidity Technique for Estimating Water Deficits in Leaves. *Australian Journal of Biological Sciences* **15**, 413-28.
- Berr A, McCallum EJ, Alioua A, Heintz D, Heitz T, Shen WH.** 2010. Arabidopsis histone methyltransferase SET DOMAIN GROUP8 mediates induction of the jasmonate/ethylene pathway genes in plant defense response to necrotrophic fungi. *Plant Physiology* **154**, 1403-14.
- Cassan O, Lèbre S, Martin A.** 2021. Inferring and analyzing gene regulatory networks from multi-factorial expression data: a complete and interactive suite. *BMC Genomics* **22**, 387.
- Chen Y, Wang Y, Huang J et al.** 2017. Salt and methyl jasmonate aggravate growth inhibition and senescence in Arabidopsis seedlings via the JA signaling pathway. *Plant Science* **261**, 1-9.
- Choudhary P, Pramitha L, Rana S, Verma S, Aggarwal PR, Muthamilarasan M.** 2021. Hormonal crosstalk in regulating salinity stress tolerance in graminaceous crops. *Physiologia Plantarum* **173**, 1587-96.
- Daudi A, O'Brien JA.** 2012. Detection of Hydrogen Peroxide by DAB Staining in Arabidopsis Leaves. *Bio Protoc* **2**, e263.
- de Ollas C, Dodd IC.** 2016. Physiological impacts of ABA-JA interactions under water-limitation. *Plant Mol Biol* **91**, 641-50.
- Delgado C, Mora-Poblete F, Ahmar S, Chen JT, Figueroa CR.** 2021. Jasmonates and Plant Salt Stress: Molecular Players, Physiological Effects, and Improving Tolerance by Using Genome-Associated Tools. *International Journal of Molecular Sciences* **22**, 3082.
- Fang C, Zhang H, Wan J et al.** 2016. Control of Leaf Senescence by an MeOH-Jasmonates Cascade that Is Epigenetically Regulated by OsSRT1 in Rice. *Molecular Plant* **9**, 1366-78.
- Feng H, Tang Q, Cai J, Xu B, Xu G, Yu L.** 2019. Rice OsHAK16 functions in potassium uptake and translocation in shoot, maintaining potassium homeostasis and salt tolerance. *Planta* **250**, 549-61.
- Formentin E, Sudiro C, Perin G et al.** 2018. Transcriptome and Cell Physiological Analyses in Different Rice Cultivars Provide New Insights Into Adaptive and Salinity Stress Responses. *Frontiers in Plant Science* **9**, 204.
- Ganie SA, Wani SH, Henry R, Hensel G.** 2021. Improving rice salt tolerance by precision breeding in a new era. *Current Opinion in Plant Biology* **60**, 101996.
- Hasanuzzaman M, Raihan MRH, Masud AAC et al.** 2021. Regulation of Reactive Oxygen Species and Antioxidant Defense in Plants under Salinity. *International Journal of Molecular Sciences* **22**, 9326.



- Hazman M, Hause B, Eiche E, Nick P, Riemann M.** 2015. Increased tolerance to salt stress in OPDA-deficient rice ALLENE OXIDE CYCLASE mutants is linked to an increased ROS-scavenging activity. *Journal of Experimental Botany* **66**, 3339-52.
- Hazman M, Sühnel M, Schäfer S et al.** 2019. Characterization of Jasmonoyl-Isoleucine (JA-Ile) Hormonal Catabolic Pathways in Rice upon Wounding and Salt Stress. *Rice (N Y)* **12**, 45.
- Heitz T.** 2021. Lipids jasmonate Metabolism: Shaping Signals for Plant Stress Adaptation and Development. In: Jez J, editor. *Encyclopedia of Biological Chemistry*. 3rd Edition. Elsevier; p. 790-803.
- Heitz T, Widemann E, Lugan R et al.** 2012. Cytochromes P450 CYP94C1 and CYP94B3 catalyze two successive oxidation steps of plant hormone Jasmonoyl-isoleucine for catabolic turnover. *Journal of Biological Chemistry* **287**, 6296-306.
- Jadamba C, Kang K, Paek NC, Lee SI, Yoo SC.** 2020. Overexpression of Rice Expansin7 (Osexpa7) Confers Enhanced Tolerance to Salt Stress in Rice. *International Journal of Molecular Sciences* **21**, E454.
- Jia Q, Li MW, Zheng C et al.** 2021. The soybean plasma membrane-localized cation/H<sup>+</sup> exchanger GmCHX20a plays a negative role under salt stress. *Physiologia Plantarum* **171**, 714-27.
- Kawasaki S, Borchert C, Deyholos M et al.** 2001. Gene expression profiles during the initial phase of salt stress in rice. *The Plant Cell* **13**, 889-905.
- Kazan K.** 2015. Diverse roles of jasmonates and ethylene in abiotic stress tolerance. *Trends in Plant Sciences* **20**, 219-29.
- Kong W, Zhong H, Gong Z et al.** 2019. Meta-Analysis of Salt Stress Transcriptome Responses in Different Rice Genotypes at the Seedling Stage. *Plants (Basel)* **8**, E64.
- Kurotani K, Hayashi K, Hatanaka S et al.** 2015a. Elevated levels of CYP94 family gene expression alleviate the jasmonate response and enhance salt tolerance in rice. *Plant Cell Physiology* **56**, 779-89.
- Kurotani K, Yamanaka K, Toda Y et al.** 2015b. Stress Tolerance Profiling of a Collection of Extant Salt-Tolerant Rice Varieties and Transgenic Plants Overexpressing Abiotic Stress Tolerance Genes. *Plant Cell Physiology* **56**, 1867-76.
- Lee S, Masclaux-Daubresse C.** 2021. Current Understanding of Leaf Senescence in Rice. *International Journal of Molecular Sciences* **22**, 4515.
- Lex A, Gehlenborg N, Strobel H, Vuilleumot R, Pfister H.** 2014. UpSet: Visualization of Intersecting Sets. *IEEE Transactions on Visualization and Computer Graphics* **20**, 1983-92.
- Li Q, Ma C, Tai H, Qiu H, Yang A.** 2020. Comparative transcriptome analysis of two rice genotypes differing in their tolerance to saline-alkaline stress. *PLoS One* **15**, e0243112.
- Liang C, Wang Y, Zhu Y et al.** 2014. OsNAP connects abscisic acid and leaf senescence by fine-tuning abscisic acid biosynthesis and directly targeting senescence-associated genes in rice. *Proc Natl Acad Sci U S A* **111**, 10013-8.
- Lim C, Kang K, Shim Y, Sakuraba Y, An G, Paek NC.** 2020. Rice ETHYLENE RESPONSE FACTOR 101 Promotes Leaf Senescence Through Jasmonic Acid-Mediated Regulation of OsNAP and OsMYC2. *Frontiers in Plant Science* **11**, 1096.
- Liu J, Zhang W, Long S, Zhao C.** 2021. Maintenance of Cell Wall Integrity under High Salinity. *International Journal of Molecular Sciences* **22**, 3260.
- Liu M, Yu H, Ouyang B et al.** 2020. NADPH oxidases and the evolution of plant salinity tolerance. *Plant, Cell & Environment* **43**, 2957-68.
- Marquis V, Smirnova E, Graindorge S et al.** 2022. Broad-spectrum stress tolerance conferred by suppressing jasmonate signaling attenuation in Arabidopsis JASMONIC ACID OXIDASE mutants. *The Plant Journal* **109**, 856-72.



- Mi H, Muruganujan A, Ebert D, Huang X, Thomas PD.** 2019. PANTHER version 14: more genomes, a new PANTHER GO-slim and improvements in enrichment analysis tools. *Nucleic Acids Research* **47**, D419-26.
- Mirdar Mansuri R, Shobbar ZS, Babaeian Jelodar N, Ghaffari MR, Nematzadeh GA, Asari S.** 2019. Dissecting molecular mechanisms underlying salt tolerance in rice: a comparative transcriptional profiling of the contrasting genotypes. *Rice (N Y)* **12**, 13.
- Muñoz P, Munné-Bosch S.** 2019. Vitamin E in Plants: Biosynthesis, Transport, and Function. *Trends in Plant Science* **24**, 1040-51.
- Nguyen TH, Mai HTT, Moukouanga D, Lebrun M, Bellafiore S, Champion A.** 2020. CRISPR/Cas9-Mediated Gene Editing of the Jasmonate Biosynthesis OsAOC Gene in Rice. *Methods in Molecular Biology* **2085**, 199-209.
- Ponce KS, Meng L, Guo L, Leng Y, Ye G.** 2021. Advances in Sensing, Response and Regulation Mechanism of Salt Tolerance in Rice. *International Journal of Molecular Sciences* **22**, 2254.
- Porra RJ, Thompson WA, Kriedemann PE.** 1989. Determination of accurate extinction coefficients and simultaneous equations for assaying chlorophylls a and b extracted with four different solvents: verification of the concentration of chlorophyll standards by atomic absorption spectroscopy. *Biochimica et Biophysica Acta (BBA)-Bioenergetics* **975**, 384-94.
- Qiu Z, Guo J, Zhu A, Zhang L, Zhang M.** 2014. Exogenous jasmonic acid can enhance tolerance of wheat seedlings to salt stress. *Ecotoxicology and Environmental Safety* **104**, 202-8.
- Raghavendra AS, Gonugunta VK, Christmann A, Grill E.** 2010. ABA perception and signalling. *Trends in Plant Science* **15**, 395-401.
- Razzaque S, Haque T, Elias SM et al.** 2017. Reproductive stage physiological and transcriptional responses to salinity stress in reciprocal populations derived from tolerant (Horkuch) and susceptible (IR29) rice. *Scientific Reports* **7**, 46138.
- Riemann M.** 2020. Phenotyping of Light Response on JA-Defective Mutant in Rice. *Methods in Molecular Biology* **2085**, 23-8.
- Riemann M, Dhakarey R, Hazman M, Miro B, Kohli A, Nick P.** 2015. Exploring Jasmonates in the Hormonal Network of Drought and Salinity Responses. *Frontiers in Plant Sciences* **6**, 1077.
- Saddhe AA, Mishra AK, Kumar K.** 2021. Molecular insights into the role of plant transporters in salt stress response. *Physiologia Plantarum* **173**, 1481-94.
- Sade N, Umnajkitikorn K, Rubio Wilhelmi MDM, Wright M, Wang S, Blumwald E.** 2018. Delaying chloroplast turnover increases water-deficit stress tolerance through the enhancement of nitrogen assimilation in rice. *Journal of Experimental Botany* **69**, 867-78.
- Sah SK, Reddy KR, Li J.** 2016. Absciscic Acid and Abiotic Stress Tolerance in Crop Plants. *Frontiers in Plant Sciences* **7**, 571.
- Tang G, Ma J, Hause B, Nick P, Riemann M.** 2020. Jasmonate is required for the response to osmotic stress in rice. *Environmental and Experimental Botany* **175**, 104047.
- Thalmann M, Santelia D.** 2017. Starch as a determinant of plant fitness under abiotic stress. *New Phytologist* **214**, 943-51.
- Toda Y, Tanaka M, Ogawa D et al.** 2013. RICE SALT SENSITIVE3 forms a ternary complex with JAZ and class-C bHLH factors and regulates jasmonate-induced gene expression and root cell elongation. *The Plant Cell* **25**, 1709-25.
- Valenzuela CE, Acevedo-Acevedo O, Miranda GS et al.** 2016. Salt stress response triggers activation of the jasmonate signaling pathway leading to inhibition of cell elongation in *Arabidopsis* primary root. *Journal of Experimental Botany* **67**, 4209-20.



- van Zelm E, Zhang Y, Testerink C.** 2020. Salt Tolerance Mechanisms of Plants. *Annual Review of Plant Biology* **71**, 403-33.
- Véry AA, Nieves-Cordones M, Daly M, Khan I, Fizames C, Sentenac H.** 2014. Molecular biology of K<sup>+</sup> transport across the plant cell membrane: what do we learn from comparison between plant species. *Journal of Plant Physiology* **171**, 748-69.
- Vishwakarma K, Upadhyay N, Kumar N et al.** 2017. Absciscic Acid Signaling and Abiotic Stress Tolerance in Plants: A Review on Current Knowledge and Future Prospects. *Frontiers in Plant Sciences* **8**, 161.
- Walia H, Wilson C, Condamine P, Liu X, Ismail AM, Close TJ.** 2007. Large-scale expression profiling and physiological characterization of jasmonic acid-mediated adaptation of barley to salinity stress. *Plant Cell and Environment* **30**, 410-21.
- Wojciechowska N, Sobieszczuk-Nowicka E, Bagniewska-Zadworna A.** 2018. Plant organ senescence - regulation by manifold pathways. *Plant Biology (Stuttg)* **20**, 167-81.
- Wu H, Ye H, Yao R, Zhang T, Xiong L.** 2015. OsJAZ9 acts as a transcriptional regulator in jasmonate signaling and modulates salt stress tolerance in rice. *Plant Science* **232**, 1-12.
- Yang C, Ma B, He SJ et al.** 2015. MAOHUZI6/ETHYLENE INSENSITIVE3-LIKE1 and ETHYLENE INSENSITIVE3-LIKE2 Regulate Ethylene Response of Roots and Coleoptiles and Negatively Affect Salt Tolerance in Rice. *Plant Physiology* **169**, 148-65.
- Yang Y, Guo Y.** 2018. Elucidating the molecular mechanisms mediating plant salt-stress responses. *New Phytologist* **217**, 523-39.
- Yu Z, Duan X, Luo L, Dai S, Ding Z, Xia G.** 2020. How Plant Hormones Mediate Salt Stress Responses. *Trends in Plant Sciences* **25**, 1117-30.
- Zhai Y, Wen Z, Fang W et al.** 2021. Functional analysis of rice OSCA genes overexpressed in the arabidopsis *osca1* mutant due to drought and salt stresses. *Transgenic Research* **30**, 811-20.
- Zhang H, Liu Y, Wen F et al.** 2014. A novel rice C2H2-type zinc finger protein, ZFP36, is a key player involved in abscisic acid-induced antioxidant defence and oxidative stress tolerance in rice. *J Exp Bot* **65**, 5795-809.
- Zhang J, Xu T, Liu Y et al.** 2022. Molecular Insights into Salinity Responsiveness in Contrasting Genotypes of Rice at the Seedling Stage. *International Journal of Molecular Sciences* **23**, 1624.
- Zhang M, Liang X, Wang L et al.** 2019. A HAK family Na<sup>+</sup> transporter confers natural variation of salt tolerance in maize. *Nature Plants* **5**, 1297-308.
- Zhao W, Wang K, Chang Y et al.** 2022. OsHyPRP06/R3L1 regulates root system development and salt tolerance via apoplastic ROS homeostasis in rice (*Oryza sativa* L.). *Plant, Cell & Environment* **45**, 900-14.
- Zou X, Liu L, Hu Z et al.** 2021. Salt-induced inhibition of rice seminal root growth is mediated by ethylene-jasmonate interaction. *Journal of Experimental Botany* **72**, 5656-72.



**Table 1**

Organ	Gene ID	TFs name	TF family	Regulation	Stress-associated function	Reference (DOI)
2 <sup>nd</sup> Leaf	<i>Os08g0481400</i>	HOX20	HALZ	down	drought tolerance	
	<i>Os01g0738400</i>	C3H10	Zinc Finger	up	drought tolerance	10.3390/plants9101298
	<i>Os03g0264600</i>	-	-	up		
	<i>Os03g0820300</i>	ZFP182	Zinc Finger	up	salt tolerance	10.1016/j.bbaexp.2007.02.006
	<i>Os05g0541400</i>	bHLH119/LF	bHLH	up		10.1093/mp/sss096
	<i>Os02g0764700</i>	ERF103	AP2	up	drought responsive	
	<i>Os06g0127100</i>	DREB1C	AP2	up		
	<i>Os08g0474000</i>	ERF104	AP2	up	drought responsive	
	<i>Os01g0859300</i>	ABI5/ABF1	bZIP_1	up	promotes salt sensitivity	10.1007/s11103-008-9298-4
	<i>Os01g0192300</i>	MYB1R1	Myb_DNA-binding	up		
	<i>Os01g0874300</i>	DLN31	Myb_DNA-binding	up		
	<i>Os02g0187700</i>	MYB1	Myb_DNA-binding	up		
	<i>Os02g0618400</i>	MPS	Myb_DNA-binding	up	cell wall remodelling	10.1111/tpj.12286
	<i>Os02g0462800</i>	WRKY42	WRKY	up	promotes leaf senescence	10.14348/molcells.2014.0128
Roots	<i>Os02g0654700</i>	ERF91/AP59	AP2	up	drought/salt tolerance	10.1104/pp.109.137554
	<i>Os09g0572000</i>	ERF87	AP2	up		
	<i>Os11g0168500</i>	ERF118	AP2	up		
	<i>Os01g0108600</i>	-	bHLH	up		
	<i>Os05g0163900</i>	bHLH036	HLH	up		
	<i>Os01g0274800</i>	CSA	Myb_DNA-binding	up		
	<i>Os01g0305900</i>	-	Myb_DNA-binding	up		
	<i>Os06g0649000</i>	WRKY28	WRKY	up	represses immune responses	10.1007/s11103-013-0032-5

**FIGURE LEGENDS**

**FIGURE 1.** JA-deficient young rice plants exhibit milder symptoms than their wild-type (WT) counterparts. Seven-day old hydroponically-grown WT and *aoc* seedlings were exposed to either control or 100 mM NaCl (salt) solutions. After 5 days, representative second (2<sup>nd</sup>) and third (3<sup>rd</sup>) leaves were photographed (a). Scale bar: 1 cm. (b) Second and 3<sup>rd</sup> leaves were detached from control and salt-exposed plants and submitted to electrolyte leakage assay. Histograms show means  $\pm$  SEM (n=5). Asterisks indicate a significant difference as determined by ANOVA plus Tukey's HSD tests (\*P < 0.05).

**FIGURE 2.** Kinetic analysis of jasmonate profile in rice seedlings submitted to 100 mM NaCl stress for 5 days. Seven-day old hydroponically-grown WT and *aoc* seedlings were exposed to either control (Control) or 100 mM NaCl (Salt) and sampled at the **time points** indicated. Roots (a) and second leaf (b) were collected separately and JAs were extracted and quantified by LC-



MS. The precursor OPDA, JA, the bioactive hormone JA-Ile and its catabolite 12COOH-JA were quantified by LC-TQMS/MS and expressed as pmol g<sup>-1</sup> fresh weight (FW). Histograms represent the mean  $\pm$  SEM of three biological replicates. For JA-Ile, hatched bars indicate signal has been detected only in one replicate. Asterisks indicate a significant difference (ANOVA plus Tukey's HSD tests \*P < 0.05; \*\*P < 0.01). LOQ: limit of quantification.

**FIGURE 3.** Transcriptome analysis of WT and *aoc* seedlings before and after salt stress. Plant samples generated as described in Figure 1 (three independent biological replicates) were used for RNA extraction and submitted to RNAseq analysis. Expression data (log<sub>2</sub> fold change) of selected genes involved in jasmonate metabolism or signaling were extracted and plotted as a heatmap for roots and 2<sup>nd</sup> leaf (a). Differentially expressed genes ( $-1 < \log_2FC < 1$ ; FDR < 0.05) were filtered in both organs and displayed as histograms with numbers of down- and up-regulated genes displayed in genotype (b) or time comparisons (c).

**FIGURE 4.** Comparative analysis of expression dynamics of genes encoding transcription factors (TFs) in WT and *aoc* roots (a) and 2<sup>nd</sup> leaf (b). Left panels: upregulated genes; right panels: downregulated genes. To screen for particular temporal behaviors, UpSet diagrams (Lex *et al.*, 2014) were utilized to display shared and genotype specific expression at different time points following salt application. Total number of TFs deregulated at a given time point in each genotype are indicated by horizontal bars. Numbers of differentially expressed TF genes ( $-1 < \log_2FC < 1$ ; FDR < 0.05) relative to 0 h are visualized as vertical bars for individual (dots) or multiple (connected dots) time points.

**FIGURE 5.** Kinetic Gene Ontology (GO) analysis of DEGs in roots (a) and 2<sup>nd</sup> leaf (b) upon salt stress. DEGs lists established in Figure 3c from each **time point** relative to 0 h were submitted to GO analysis on Panther classification system to retrieve Biological processes significantly enriched within each DEGs list (FDR < 0.01). GO terms for upregulated DEGs: upper panels, red scale; GO terms for downregulated DEGs: lower panels, blue scale)

**FIGURE 6.** Analysis of ABA pathway genes, hormone content and water management responses upon salt stress in rice. Expression heatmap of described rice ABA metabolic genes is shown for *aoc* and WT roots and 2<sup>nd</sup> leaf (a). ABA content in roots and 3<sup>rd</sup> leaf. Histograms show the mean of 3 independent biological replicates  $\pm$  SEM; \*P < 0.05 (b). Expression heatmap of genes associated with GO term “response to water deprivation”. Only genes whose



expression was changed at least at one time point in *aoc* or WT ( $-1 < \log_2FC < 1$ ;  $FDR < 0.05$ ) are represented (c). Stomatal conductance to water vapor (gsw) was determined in leaf 5 of WT and *aoc* plants (d, left panel). Relative water content (RWC) was determined in 3<sup>rd</sup> leaf of WT and *aoc* plants submitted to salt stress for 4 days (d; right panel). Histograms represent the mean of 3 (gsw) or 4 (RWC) biological replicates  $\pm$  SEM. Asterisks indicate a significant difference (ANOVA plus Tukey's HSD tests, \* $P < 0.05$ ; \*\* $P < 0.01$ ; \*\*\* $P < 0.001$ ).

**FIGURE 7.** Analysis of differential ion transporter gene expression and ion accumulation in roots and leaves upon salt stress. Expression profiles of ion transporter genes in *aoc* vs WT are represented as kinetic heatmaps (a). Only transporter genes whose expression was changed at least at one time point in *aoc* or WT ( $-1 < \log_2FC < 1$ ;  $FDR < 0.05$ ) are represented. Expression of *HAK4* transporter gene in roots of WT plants exposed to MeJA. Data are taken from RiceXpro database (b). Quantification of  $Na^+$  and  $K^+$  ion accumulation in roots, 2<sup>nd</sup> and 3<sup>rd</sup> leaves: means  $\pm$  SEM from 6 independent biological replicates are represented (c). Asterisks indicate a significant difference (ANOVA plus Tukey's HSD tests, \* $P < 0.05$ ; \*\* $P < 0.01$ ; \*\*\* $P < 0.001$ ).

**FIGURE 8.** Analysis of reactive oxygen species-scavenging systems in leaves under salt stress. Second leaves of *aoc* or WT seedlings were submitted to DAB staining to visualize extent of  $H_2O_2$  accumulation (a). Genotype comparison (*aoc* vs WT) of differentially-expressed genes encoding ROS-scavenging activities. APX: ascorbate peroxidase; FSD: iron-dependent superoxide dismutase; GST: glutathione S-transferase; SOD: superoxide dismutase (b). Expression of *FSD1.1* and *FSD1.2* in leaves of WT plants exposed to MeJA (c). Asterisks indicate a significant difference (ANOVA plus Tukey's HSD tests, \* $P < 0.05$ ; \*\* $P < 0.01$ ; \*\*\* $P < 0.001$ ).

**FIGURE 9.** Jasmonate deficiency delays induction of senescence-promoting genes upon salt stress. Expression of genes associated with senescence (SAGs) was compared in 2<sup>nd</sup> leaf between *aoc* and WT genotypes at four time points and genes whose expression was changed at least at one time point in either genotype ( $-1 < \log_2FC < 1$ ;  $FDR < 0.05$ ) are represented as a kinetic heatmap (a). Expression of *OsI43* and *OsNAP*, two SAGs that are strongly differential in (a), was monitored upon response to MeJA exposure (b). Histograms display means  $\pm$  SEM from 3 biological replicates. Chlorophyll contents was determined in WT and *aoc* 2<sup>nd</sup> or 3<sup>rd</sup>



leaves after 4 days of salt stress (c). Asterisks indicate a significant difference in means (ANOVA plus Tukey's HSD tests, \* $P < 0.05$ ; \*\* $P < 0.01$ ; \*\*\* $P < 0.001$ ).

**FIGURE 10.** Proposed model of JA-regulated functions in the rice response to salt stress. The study links newly-defined JAs gene targets to specific impacts of JA signaling on the salinity response physiology. Salt stress through its successive osmotic and ionic components stimulates JA metabolism which leads to waves of transcriptional changes with organ-specific temporal patterns. Root response is immediate-early while in shoot a bi-phasic response is discerned at hormonal and transcriptional levels. ABA responses are largely JA-independent in root, but JA signaling is critical for full induction of ABA biosynthetic genes and ABA accumulation in shoot. Both hormones synergistically activate ABA-regulated responses including dehydrins and RAB genes to boost water retention, including reduction of stomatal conductance and water loss in rice leaves. On the other hand, JA signaling, through transcriptional repression of *HAK4* in roots and *FSD* genes in leaves, impairs  $\text{Na}^+$  exclusion from root xylem and ROS detoxification in leaves respectively, which aggravates  $\text{Na}^+$  toxicity in photosynthetic tissues. This set of responses, associated with the induction by JAs of *NAP*, a transcriptional activator of leaf senescence, can explain the severe necrotic symptoms observed in WT leaves after salt stress. The findings establish JAs as multifaceted regulators of the rice salt stress response, where JA signaling can no longer be uniformly associated with salt sensitivity or tolerance. Black arrows and red lines indicate transcriptional activation and repression of JA-target genes respectively; compiled “greater than” symbols indicate positive regulation of key pathways involved in rice salt stress response. h: hours. d: days.

**TABLE 1:** List of transcription factor (TF) genes coregulated with JA pathway genes in rice salt stress response. Genes were selected from data in Figure 4 on the basis of their exclusive regulation in WT at 1 h and 6 h for roots, or 1 h and 72 h for shoot, and their absence of response in *aoc* ( $-1 < \log_2\text{FC} < 1$ ;  $\text{FDR} < 0.05$ ).



**Figure 1**

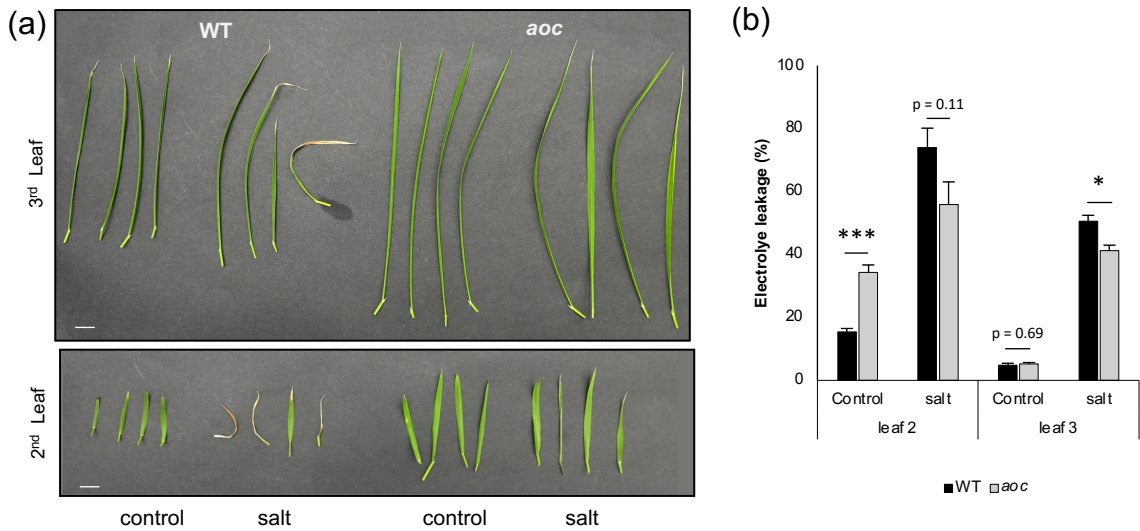


**FIGURE 1.** JA-deficient young rice plants exhibit milder symptoms than their wild-type (WT) counterparts. Seven-day old hydroponically-grown WT and *aoc* seedlings were exposed to either control or 100 mM NaCl (salt) solutions. After 5 days, representative second (2<sup>nd</sup>) and third (3<sup>rd</sup>) leaves were photographed (a). Scale bar: 1 cm. (b) Second and 3<sup>rd</sup> leaves were detached from control and salt-exposed plants and submitted to electrolyte leakage assay. Histograms show means  $\pm$  SEM (n=5). Asterisks indicate a significant difference as determined by ANOVA plus Tukey's HSD test (\*P < 0.05).



**Figure 2**

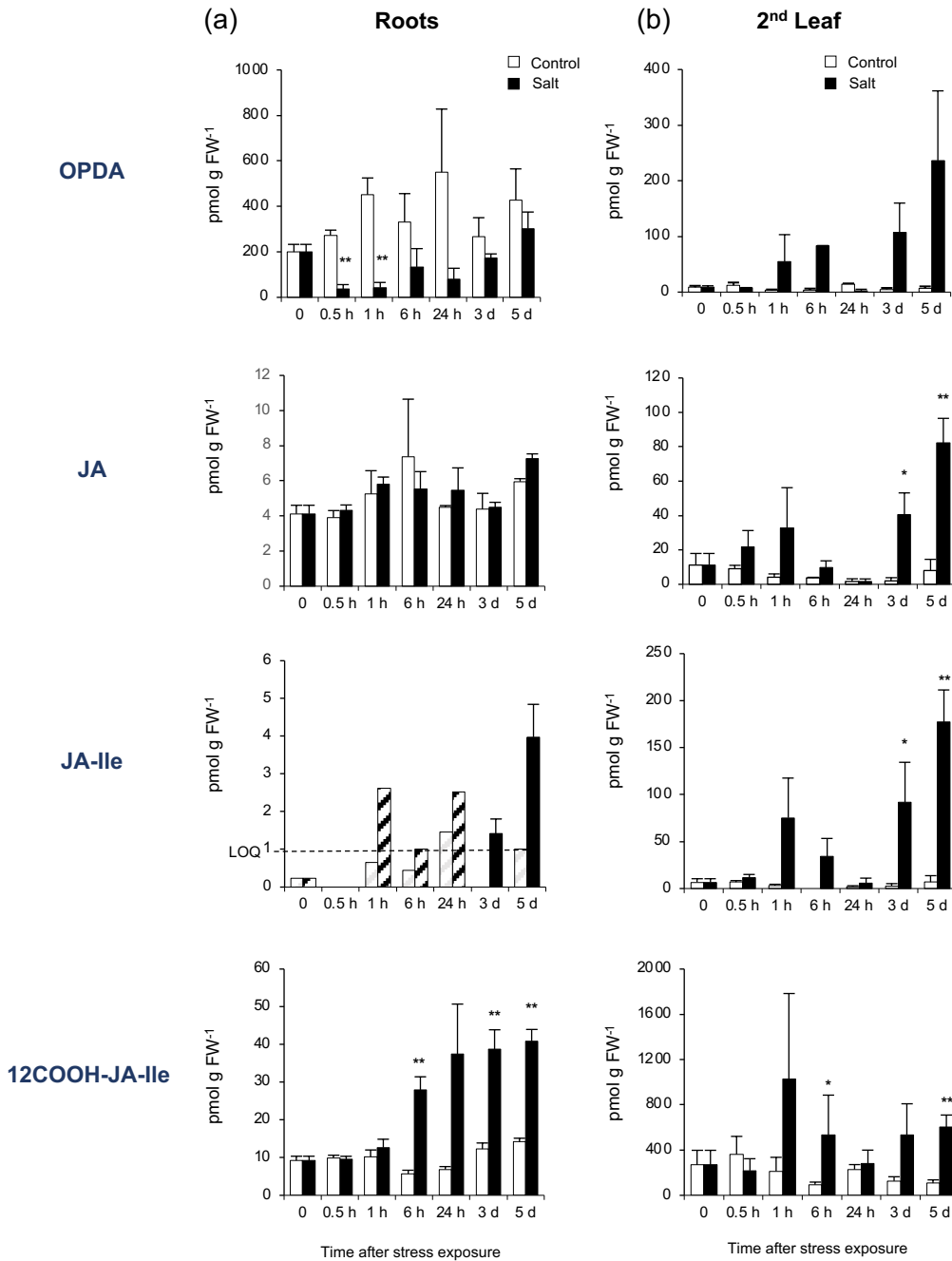


**FIGURE 2.** Kinetic analysis of jasmonate profile in rice seedlings submitted to 100 mM NaCl stress for 5 days. Seven-day old hydroponically-grown WT and *aoc* seedlings were exposed to either control (Control) or 100 mM NaCl (Salt) and sampled at the time points indicated. Roots (a) and second leaf (b) were collected separately and JAs were extracted and quantified. The precursor OPDA, JA, the bioactive hormone JA-Ile and its catabolite 12COOH-JA-Ile were quantified by LC-MS/MS and expressed as pmol g<sup>-1</sup> fresh weight (FW). Histograms represent the mean  $\pm$  SEM of three biological replicates. For JA-Ile, hatched bars indicate signal has been detected only in one replicate. Asterisks indicate a significant difference (ANOVA plus Tukey's HSD tests \*P < 0.05; \*\*P < 0.01). LOQ : limit of quantification.



Figure 3

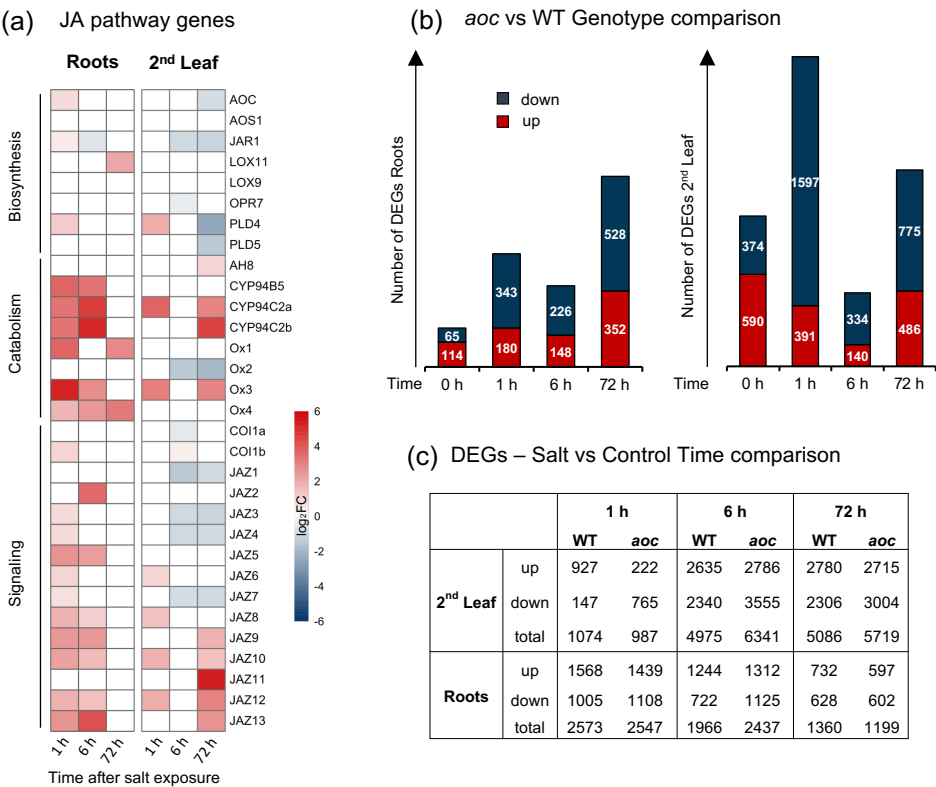


**FIGURE 3.** Transcriptome analysis of WT and *aoc* seedlings before and after salt stress. Plant samples generated as described in Figure 1 (three independent biological replicates) were used for RNA extraction and submitted to RNAseq analysis. Expression data (log<sub>2</sub> fold change) of selected genes involved in jasmonate metabolism or signaling were extracted and plotted as a heatmap for roots and 2<sup>nd</sup> leaf (a). Differentially expressed genes ( $-1 < \log_2FC < 1$ ; FDR < 0.05) were filtered in both organs and displayed as histograms with numbers of down- and up-regulated genes displayed in genotype (b) or time comparisons (c).



**Figure 4**

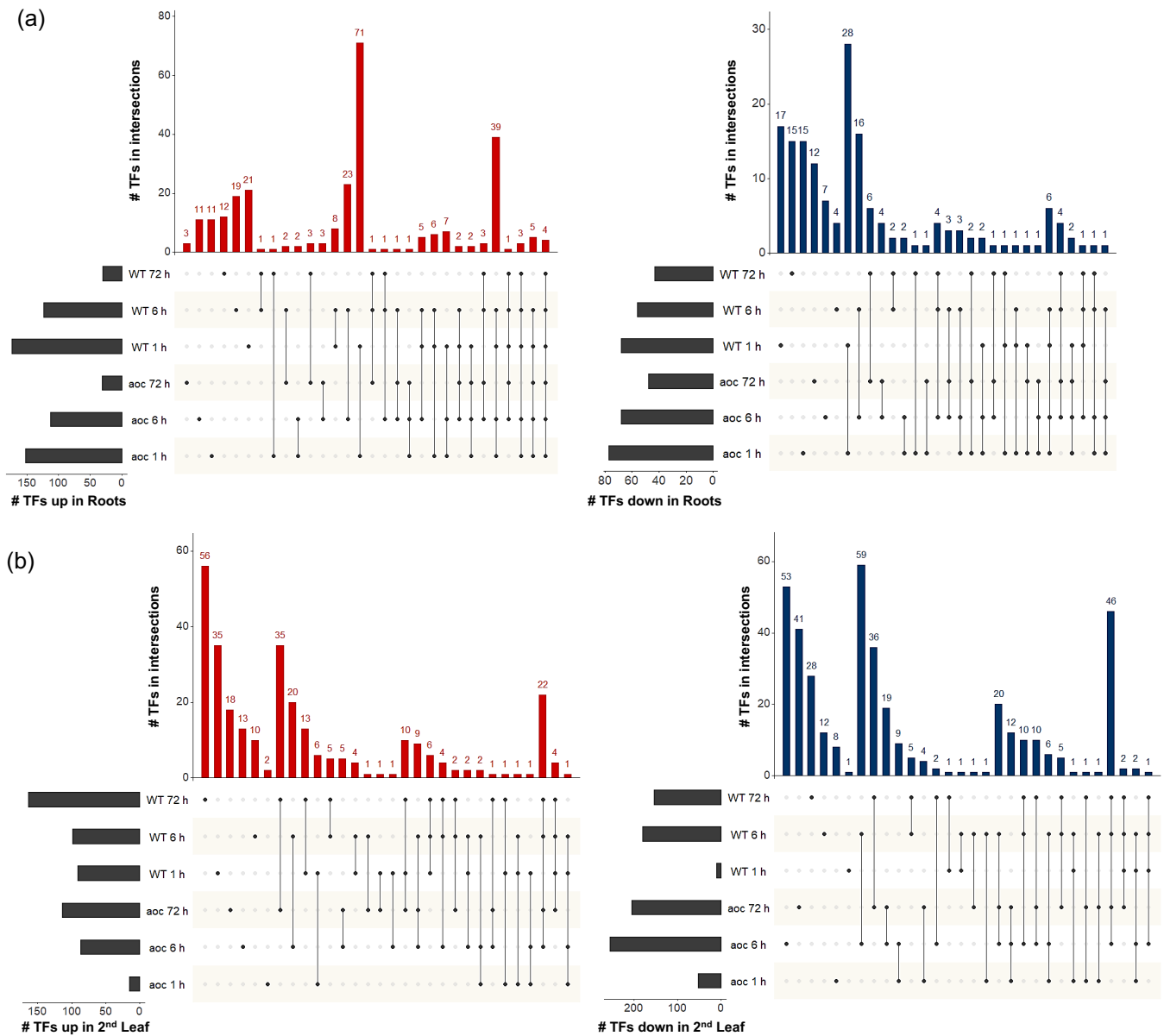


**FIGURE 4.** Comparative analysis of expression dynamics of genes encoding transcription factors (TFs) in WT and *aoc* roots (a) and 2<sup>nd</sup> leaf (b). Left panels: upregulated genes; right panels: downregulated genes. To screen for particular temporal behaviors, UpSet diagrams (Lex et al., 2014) were utilized to display shared and genotype specific expression at different time points following salt application. Total number of TFs deregulated at a given time point in each genotype are indicated by horizontal bars. Numbers of differentially expressed TF genes ( $-1 < \log_2FC < 1$ ; FDR < 0.05) relative to 0 h are visualized as vertical bars for individual (dots) or multiple (connected dots) time points.



**Table 1**

Organ	Gene ID	TFs name	TF family	Regulation	Stress-associated function	Reference (DOI)
2 <sup>nd</sup> Leaf	Os08g0481400	HOX20	HALZ	down	drought tolerance	
	Os01g0738400	C3H10	Zinc Finger	up	drought tolerance	10.3390/plants9101298
	Os03g0264600	-	-	up		
	Os03g0820300	ZFP182	Zinc Finger	up	salt tolerance	10.1016/j.bbaexp.2007.02.006
	Os05g0541400	bHLH119/LF	bHLH	up		10.1093/mp/sss096
	Os02g0764700	ERF103	AP2	up	drought responsive	
	Os06g0127100	DREB1C	AP2	up		
	Os08g0474000	ERF104	AP2	up	drought responsive	
	Os01g0859300	ABI5/ABF1	bZIP_1	up	promotes salt sensitivity	10.1007/s11103-008-9298-4
	Os01g0192300	MYB1R1	Myb_DNA-binding	up		
	Os01g0874300	DLN31	Myb_DNA-binding	up		
	Os02g0187700	MYB1	Myb_DNA-binding	up		
	Os02g0618400	MPS	Myb_DNA-binding	up	cell wall remodelling	10.1111/tpj.12286
	Os02g0462800	WRKY42	WRKY	up	promotes leaf senescence	10.14348/molcells.2014.0128
Roots	Os02g0654700	ERF91/AP59	AP2	up	drought/salt tolerance	10.1104/pp.109.137554
	Os09g0572000	ERF87	AP2	up		
	Os11g0168500	ERF118	AP2	up		
	Os01g0108600	-	bHLH	up		
	Os05g0163900	bHLH036	HLH	up		
	Os01g0274800	CSA	Myb_DNA-binding	up		
	Os01g0305900	-	Myb_DNA-binding	up		
	Os06g0649000	WRKY28	WRKY	up	represses immune responses	10.1007/s11103-013-0032-5

**TABLE 1:** List of transcription factor (TF) genes coregulated with JA pathway genes in rice salt stress response. Genes were selected from data in Figure 4 on the basis of their exclusive regulation in WT at 1 h and 6 h for roots, or 1 h and 72 h for shoot, and their absence of response in *aoc* ( $-1 < \log_2FC < 1$ ; FDR < 0.05).



Figure 5

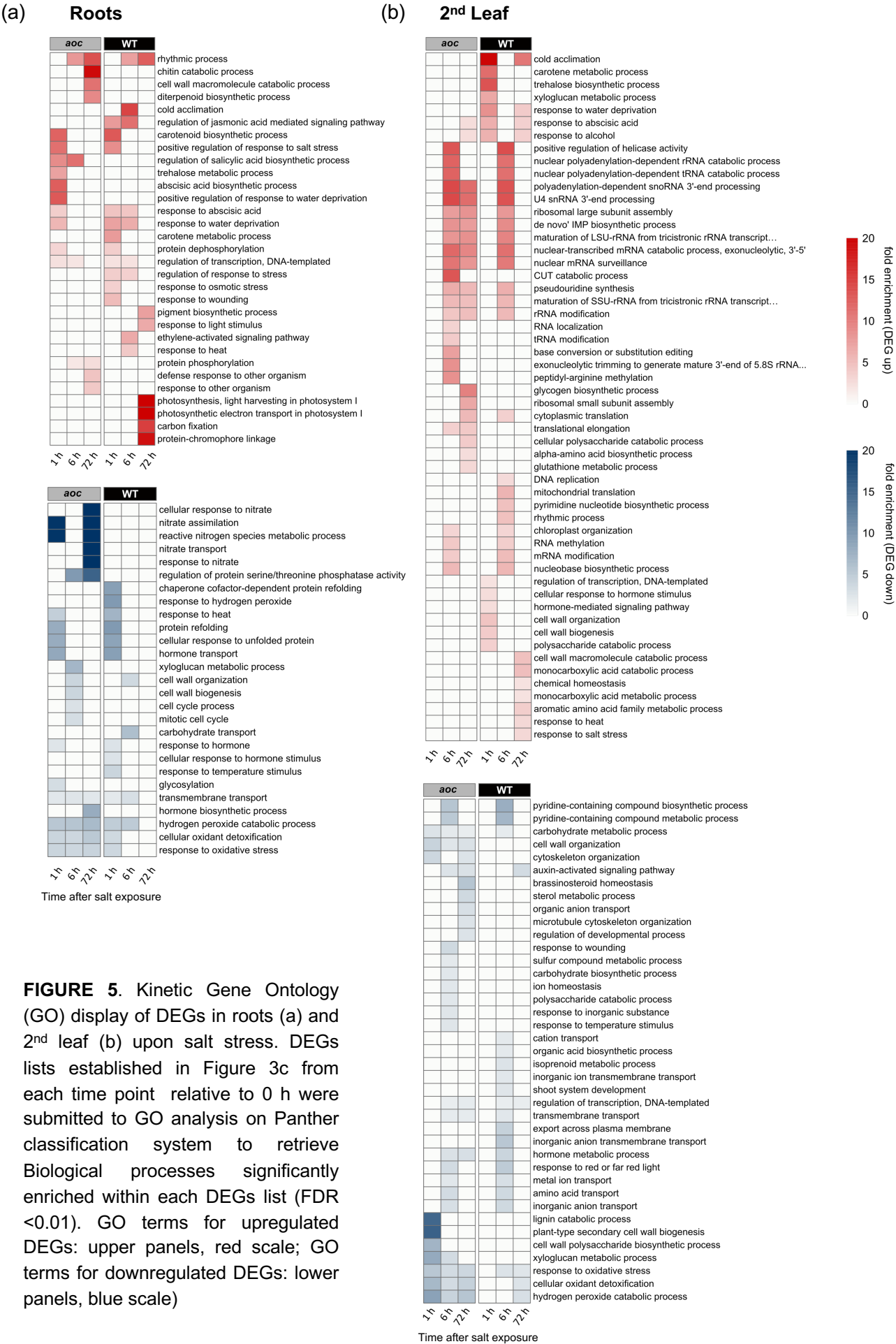


**FIGURE 5.** Kinetic Gene Ontology (GO) display of DEGs in roots (a) and 2<sup>nd</sup> leaf (b) upon salt stress. DEGs lists established in Figure 3c from each time point relative to 0 h were submitted to GO analysis on Panther classification system to retrieve Biological processes significantly enriched within each DEGs list (FDR <0.01). GO terms for upregulated DEGs: upper panels, red scale; GO terms for downregulated DEGs: lower panels, blue scale)



**Figure 6**

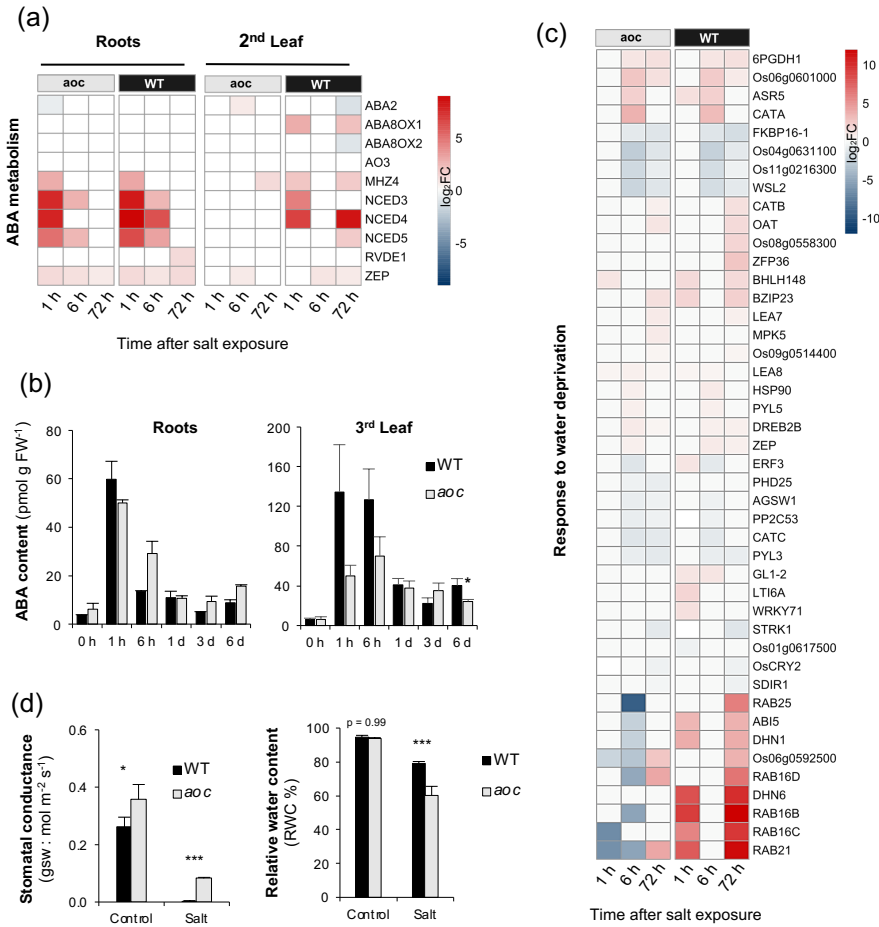


**FIGURE 6.** Analysis of ABA pathway genes, hormone content and water management responses upon salt stress in rice. Expression heatmap of described rice ABA metabolic genes is shown for *aoc* and WT roots and 2<sup>nd</sup> leaf (a). ABA content in roots and 3<sup>rd</sup> leaf. Histograms show the mean of 3 independent biological replicates  $\pm$  SEM; \* $P < 0.05$  (b). Expression heatmap of genes associated with GO term “response to water deprivation”. Only genes whose expression was changed at least at one time point in *aoc* or WT ( $-1 < \log_2FC < 1$ ; FDR  $< 0.05$ ) are represented (c). Stomatal conductance to water vapor (gs) was determined in leaf 5 of WT and *aoc* plants (d, left panel). Relative water content (RWC) was determined in 3<sup>rd</sup> leaf of WT and *aoc* plants submitted to salt stress for 4 days (d; right panel). Histograms represent the mean of 3 (gs) or 4 (RWC) biological replicates  $\pm$  SEM. Asterisks indicate a significant difference (ANOVA plus Tukey’s HSD tests, \* $P < 0.05$ ; \*\* $P < 0.01$ ; \*\*\* $P < 0.001$ ).



**Figure 7**

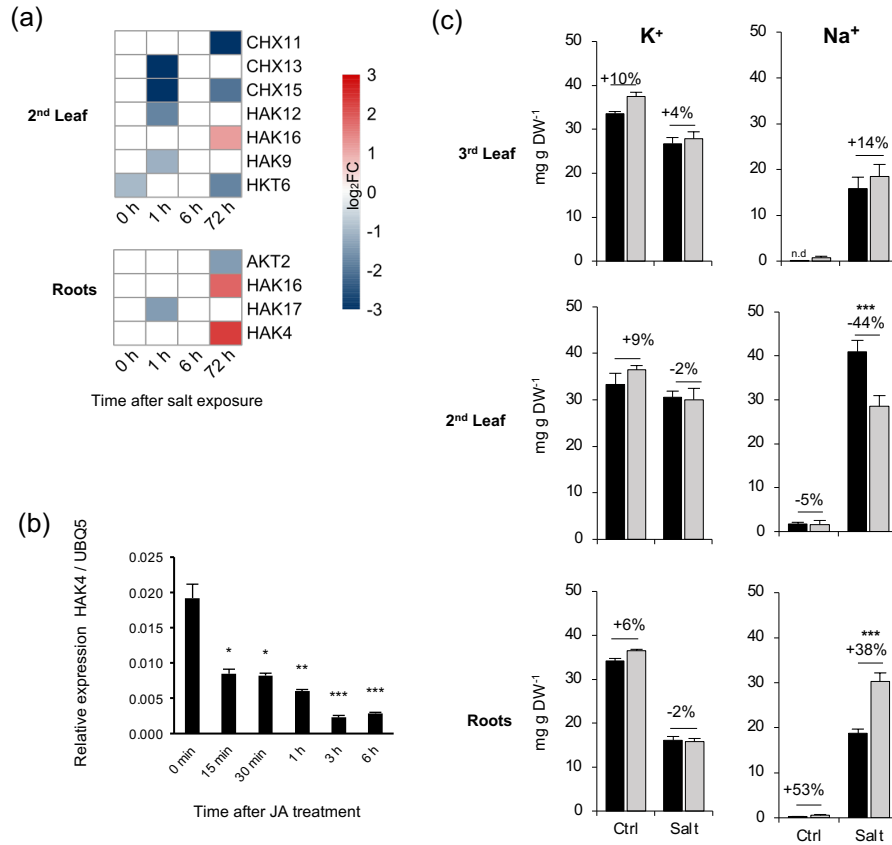


**FIGURE 7.** Analysis of differential ion transporter gene expression and ion accumulation in roots and leaves upon salt stress. Expression profiles of ion transporter genes in *aoc* vs WT are represented as kinetic heatmaps (a). Only transporter genes whose expression was changed at least at one time point in *aoc* or WT ( $-1 < \log_2 FC < 1$ ; FDR < 0.05) are represented. Expression of *HAK4* transporter gene in roots of WT plants exposed to MeJA. Data are taken from RiceXpro database (b). Quantification of Na<sup>+</sup> and K<sup>+</sup> ion accumulation in roots, 2<sup>nd</sup> and 3<sup>rd</sup> leaves : means  $\pm$  SEM from 6 independent biological replicates are represented (c). Asterisks indicate a significant difference (ANOVA plus Tukey's HSD tests, \*P < 0.05; \*\*P < 0.01; \*\*\*P < 0.001).



**Figure 8**

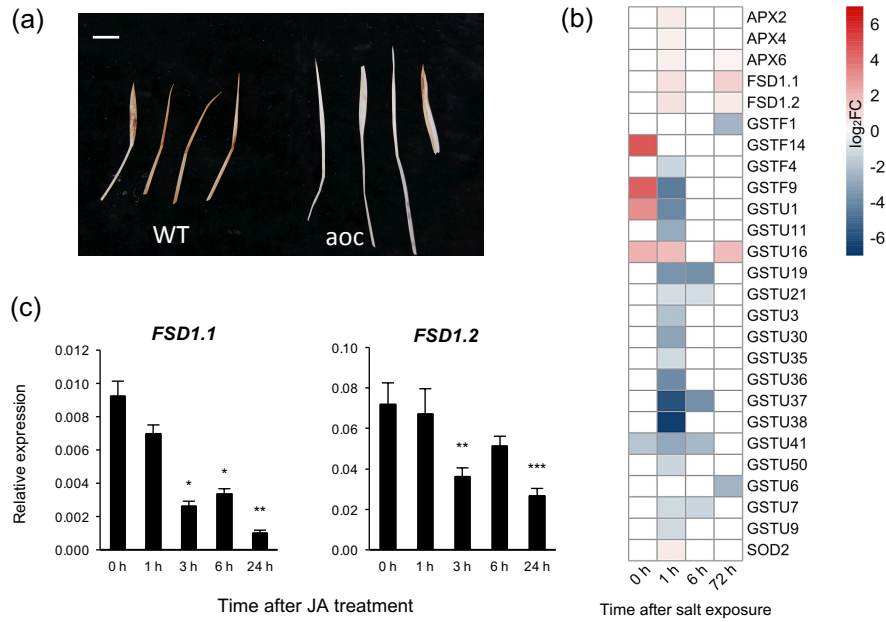


**FIGURE 8.** Analysis of reactive oxygen species-scavenging systems in leaves under salt stress. Second leaves of *aoc* or WT seedlings were submitted to DAB staining to visualize extent of H<sub>2</sub>O<sub>2</sub> accumulation. Scale bar: 1 cm (a). Genotype comparison (*aoc* vs WT) of differentially-expressed genes encoding ROS-scavenging activities. APX : ascorbate peroxidase; FSD: iron-dependent superoxide dismutase; GST: glutathione S-transferase; SOD: superoxide dismutase (b). Expression of *FSD1.1* and *FSD1.2* in leaves of WT plants exposed to MeJA (c). Asterisks indicate a significant difference (ANOVA plus Tukey's HSD tests, \*P < 0.05; \*\*P < 0.01; \*\*\*P < 0.001).



**Figure 9**

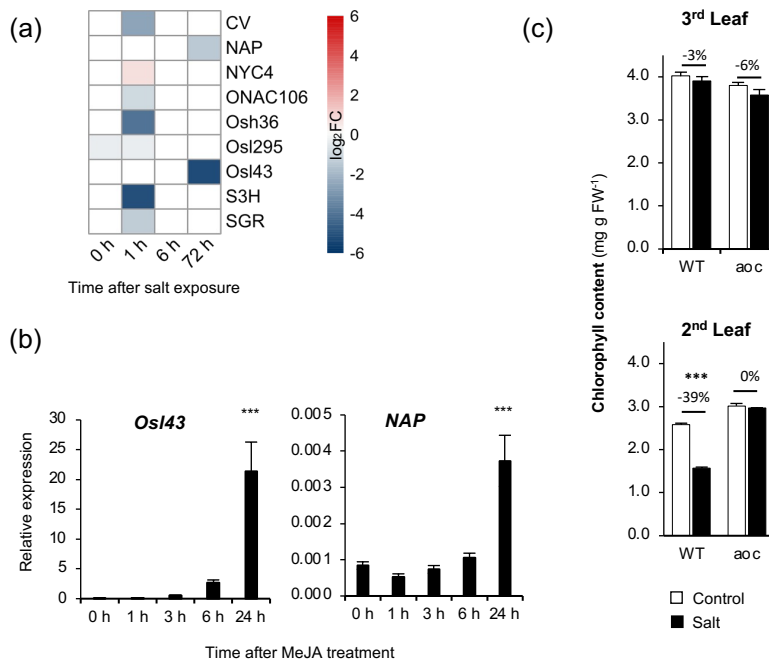


**FIGURE 9.** Jasmonate deficiency delays induction of senescence-promoting genes upon salt stress. Expression of genes associated with senescence (SAGs) was compared in 2<sup>nd</sup> leaf between *aoc* and WT genotypes at four time points and genes whose expression was changed at least at one time point in either genotype ( $-1 < \log_2FC < 1$ ; FDR < 0.05) are represented as a kinetic heatmap (a). Expression of *OsI43* and *OsNAP*, two SAGs that are strongly differential in (a), was monitored upon response to MeJA exposure (b). Histograms display means  $\pm$  SEM from 3 biological replicates. Chlorophyll contents was determined in WT and *aoc* 2<sup>nd</sup> or 3<sup>rd</sup> leaves after 4 days of salt stress (c). Asterisks indicate a significant difference in means (ANOVA plus Tukey's HSD tests, \*P < 0.05; \*\*P < 0.01; \*\*\*P < 0.001).



Figure 10

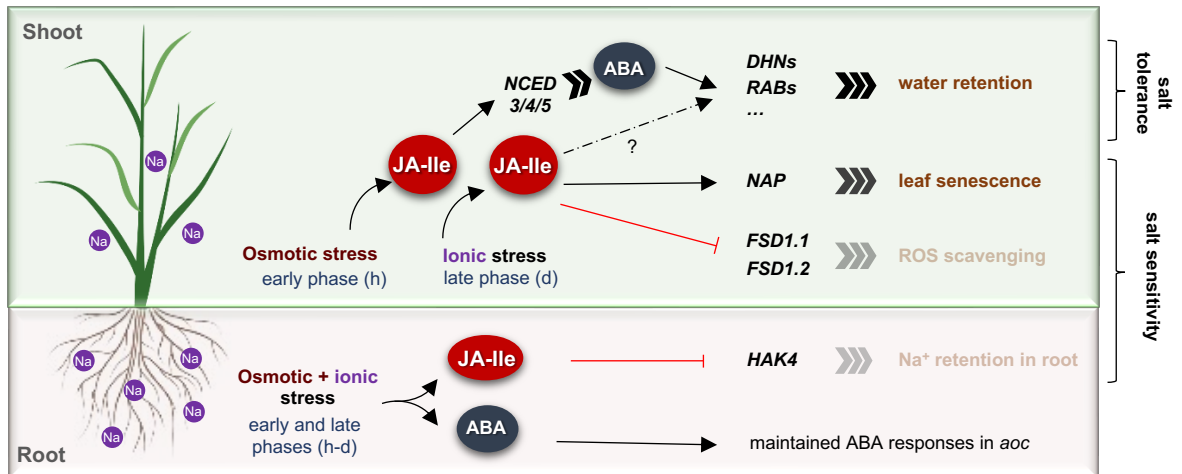


**FIGURE 10. Proposed model of JA-regulated functions in the rice response to salt stress.** The study links newly-defined JAs gene targets to specific impacts of JA signaling on the salinity response physiology. Salt stress through its successive osmotic and ionic components stimulates JA metabolism which leads to waves of transcriptional changes with organ-specific temporal patterns. Root response is immediate-early while in shoot a bi-phasic response is discerned at hormonal and transcriptional levels. ABA responses are largely JA-independent in root, but JA signaling is critical for full induction of ABA biosynthetic genes and ABA accumulation in shoot. Both hormones synergistically activate ABA-regulated responses including dehydrins and RAB genes to boost water retention, including reduction of stomatal conductance and water loss in rice leaves. On the other hand, JA signaling, through transcriptional repression of *HAK4* in roots and *FSD* genes in leaves, impairs Na<sup>+</sup> exclusion from root xylem and ROS detoxification in leaves respectively, which aggravates Na<sup>+</sup> toxicity in photosynthetic tissues. This set of responses, associated with the induction by JAs of *NAP*, a transcriptional activator of leaf senescence, can explain the severe necrotic symptoms observed in WT leaves after salt stress. The findings establish JAs as multifaceted regulators of the rice salt stress response, where JA signaling can no longer be uniformly associated with salt sensitivity or tolerance. Black arrows and red lines indicate transcriptional activation and repression of JA-target genes respectively; compiled “greater than” symbols indicate positive regulation of key pathways involved in rice salt stress response. h: hours. d: days.



**Figure S1**

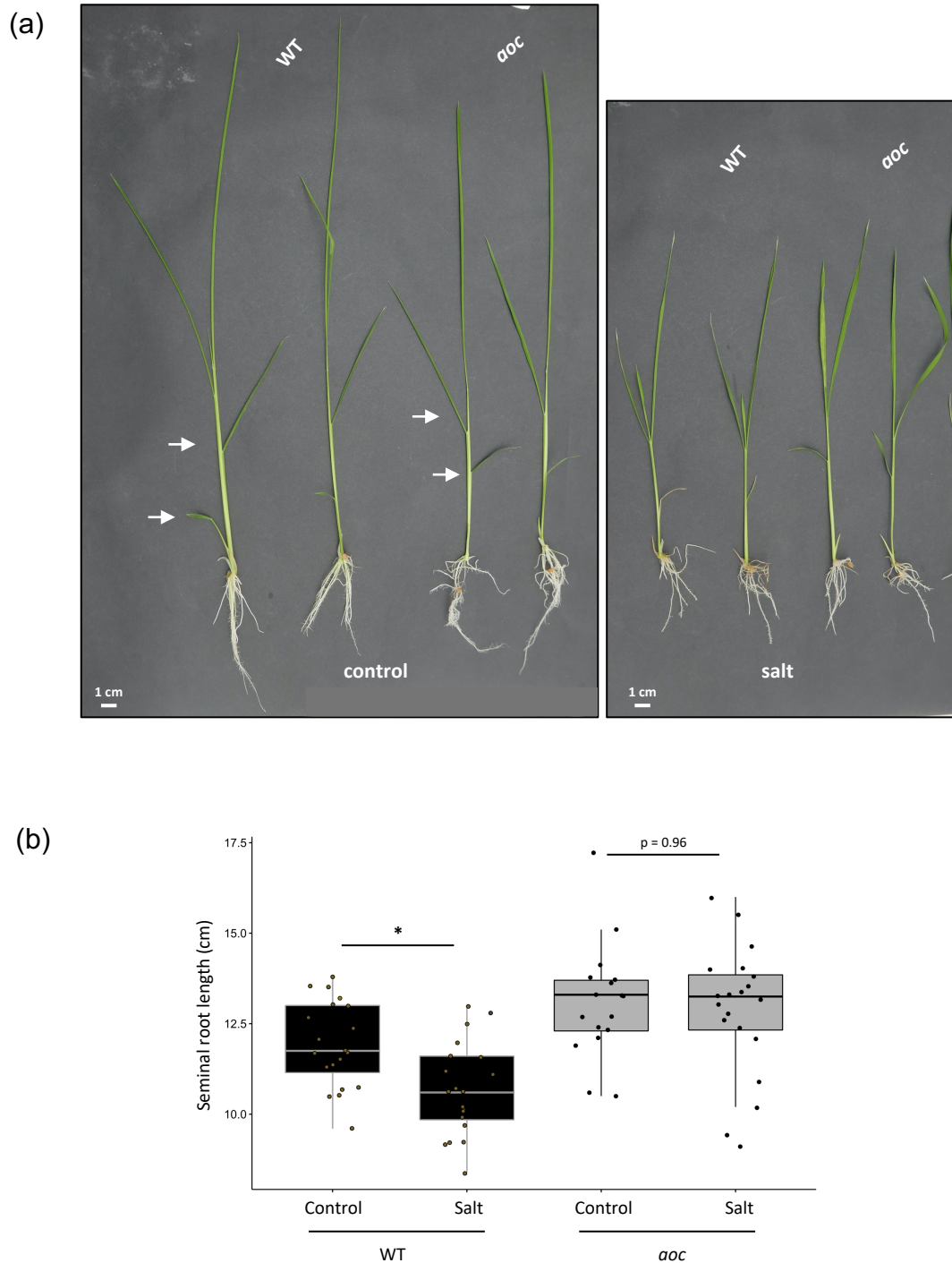
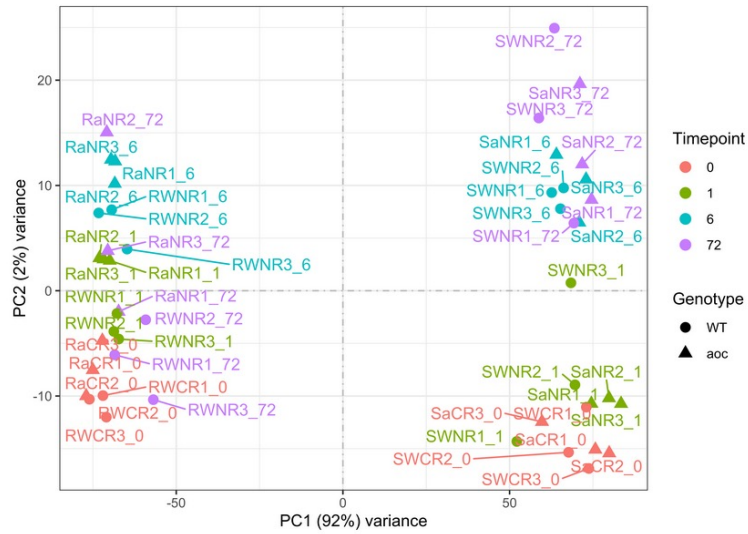


**FIGURE S1.** Developmental phenotypes of rice wild-type (WT) and jasmonate-deficient (*aoc*) seedlings exposed to control or 100 mM NaCl (salt) solutions. Two representative plants from each condition were photographed 5 days after exposure. Arrows on control plants designate second (lower) and third leaves (a). Seminal root length was measured and represented in boxplots with  $n = 20$  (except *aoc*-control,  $n = 17$ ) (b). Asterisk \* indicates significant difference (ANOVA plus Tukey's HSD tests,  $*P < 0.05$ ).

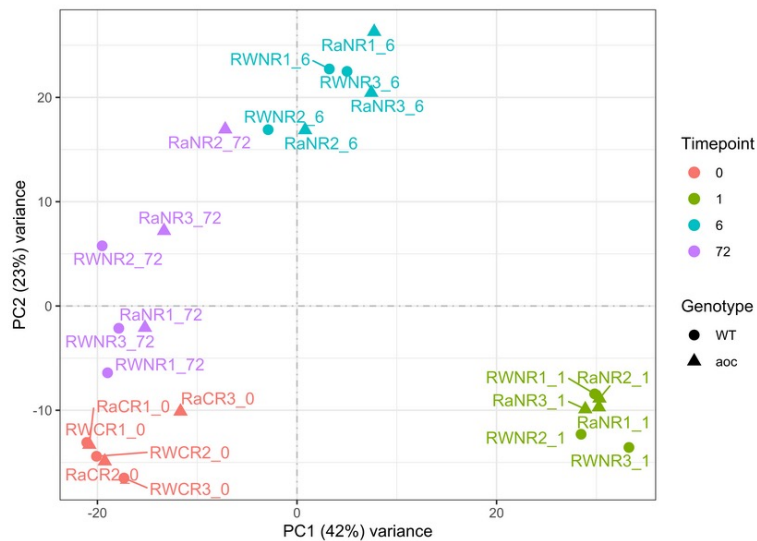


**Figure S2**

(a) Global



(b) Roots



(c) 2<sup>nd</sup> Leaf

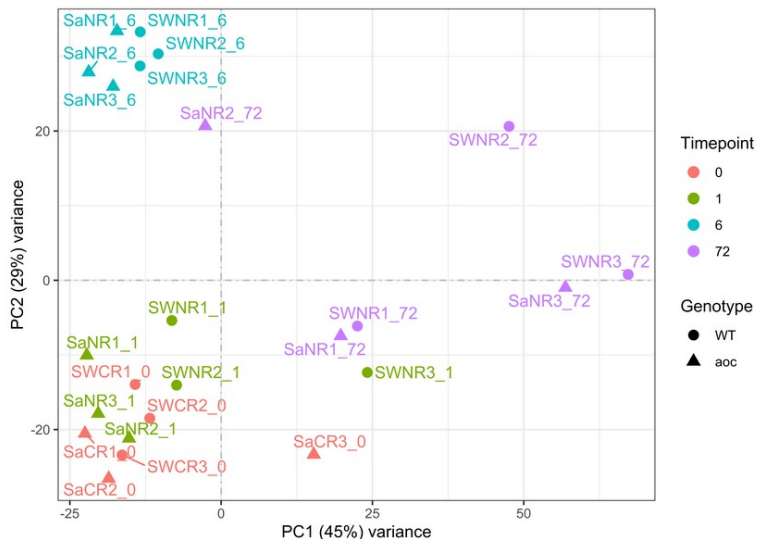


**FIGURE S2.** Principal component analysis (PCA) of RNAseq data distribution. Global normalization was applied to root and 2<sup>nd</sup> leaf samples (Total of 48 samples with each biological condition in 3 independent replicates (a). Sample designation: R or S = Root or Shoot; W or a = WT or aoc; Rx = replicate number. Root samples only (24) were normalized and analyzed in (b). 2<sup>nd</sup> leaf samples only (24) were normalized and analyzed in (c).



Figure S3

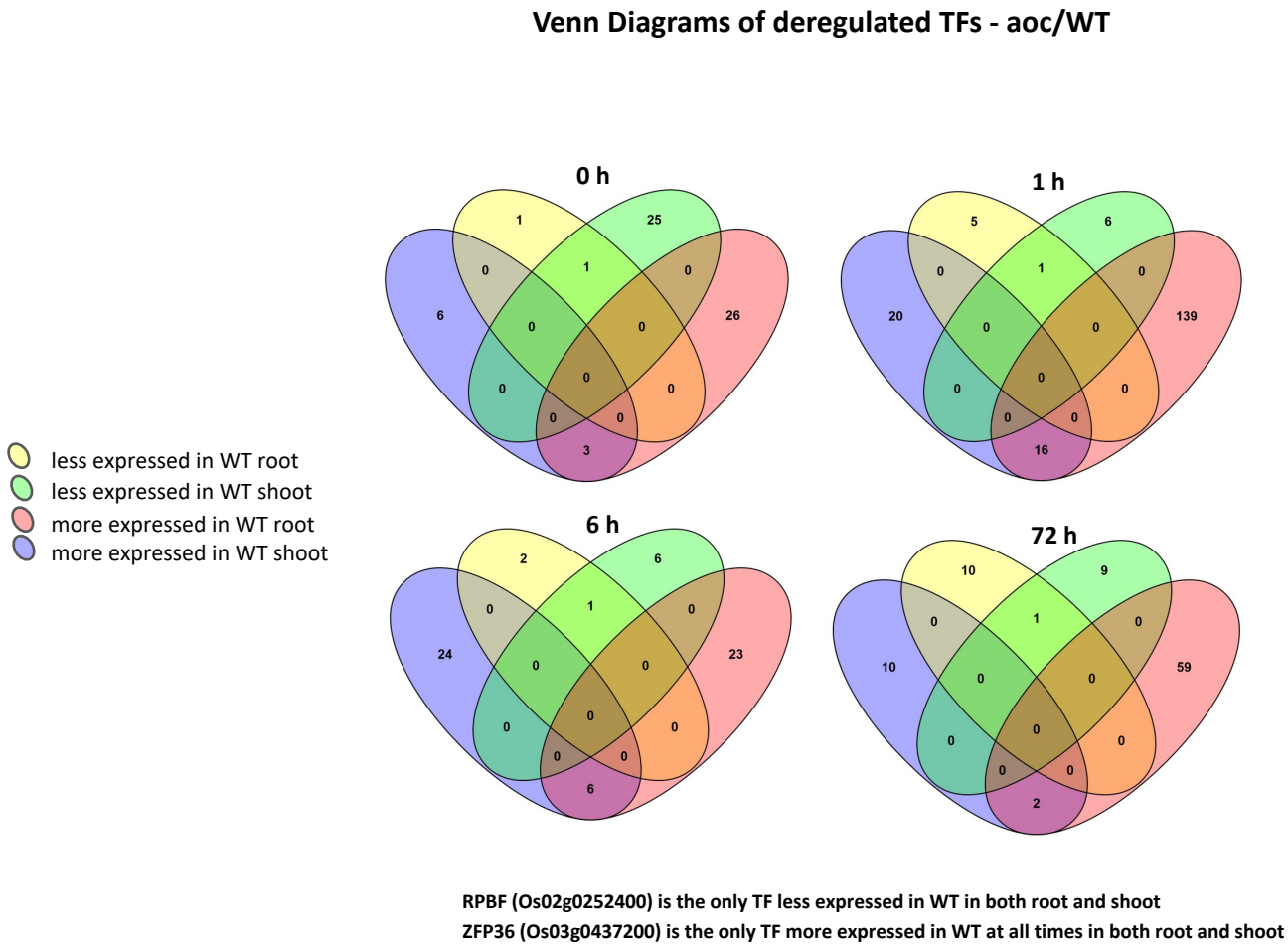
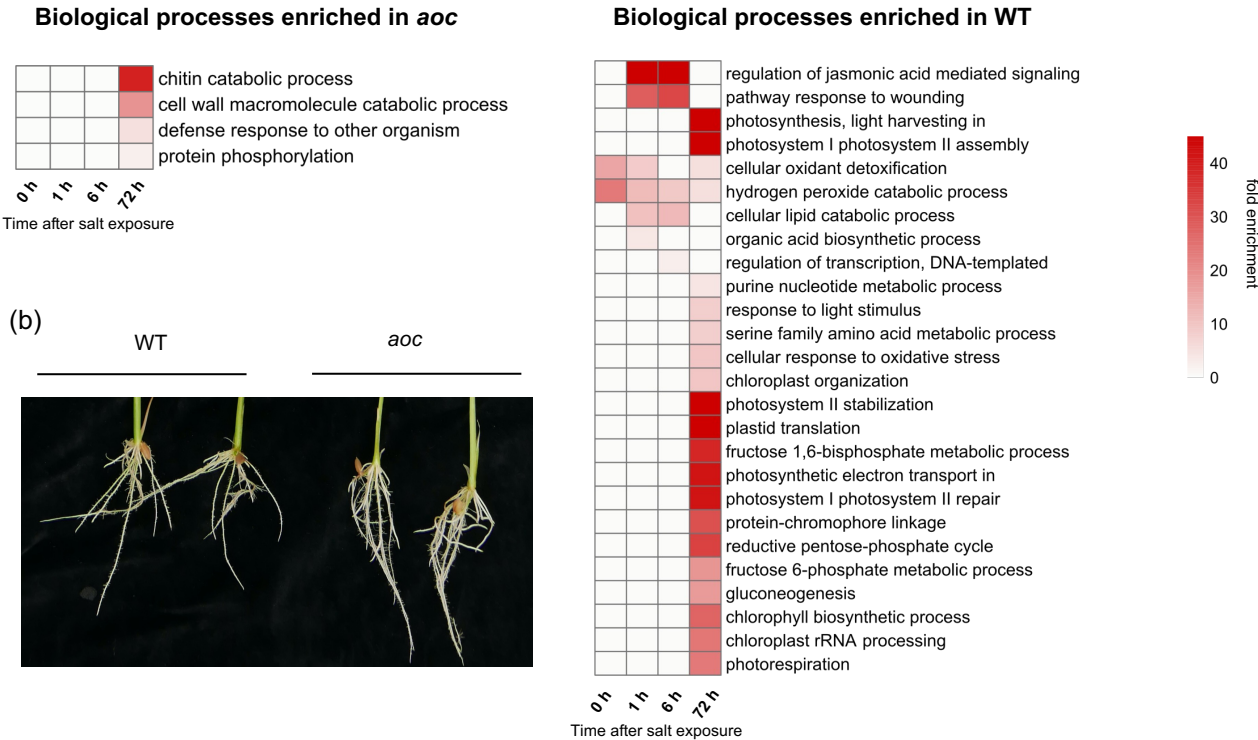


**FIGURE S3.** Analysis of extent of overlap between deregulated transcription factor (TF) genes in shoot and root. Lists of genes showing differential expression in each organ in the *aoc*/WT comparison were crossed for each of the 4 timepoints (h) of salt response. Number of genes in common between the two organs comparisons are represented in Venn diagrams.



**Figure S4**

**(a) Roots**



**(c) 2<sup>nd</sup> Leaf**

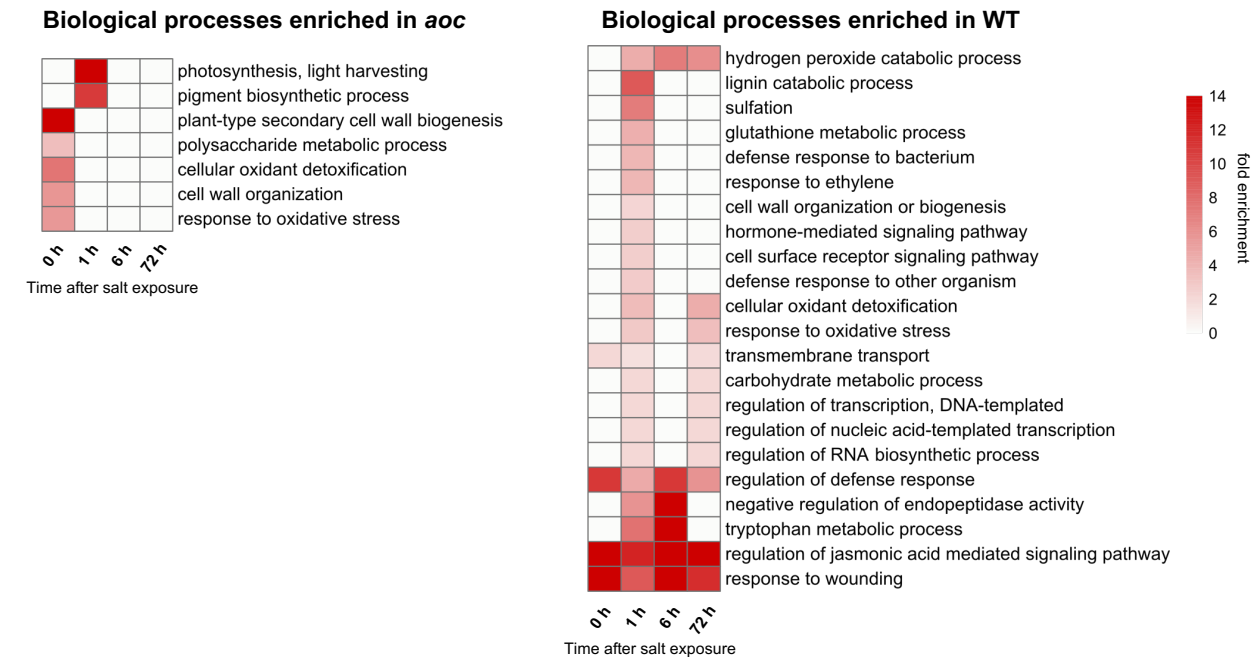


**FIGURE S4.** Gene ontology (GO) analysis of differentially expressed genes (DEGs). DEG lists at each time point relative to 0 h were submitted to GO analysis and enrichment of biological processes (FDR < 0.01) in *aoc* or WT was displayed as heatmaps for roots (a) and 2<sup>nd</sup> leaf (c). Roots were photographed at 6 days after exposure (b).



**Figure S5**

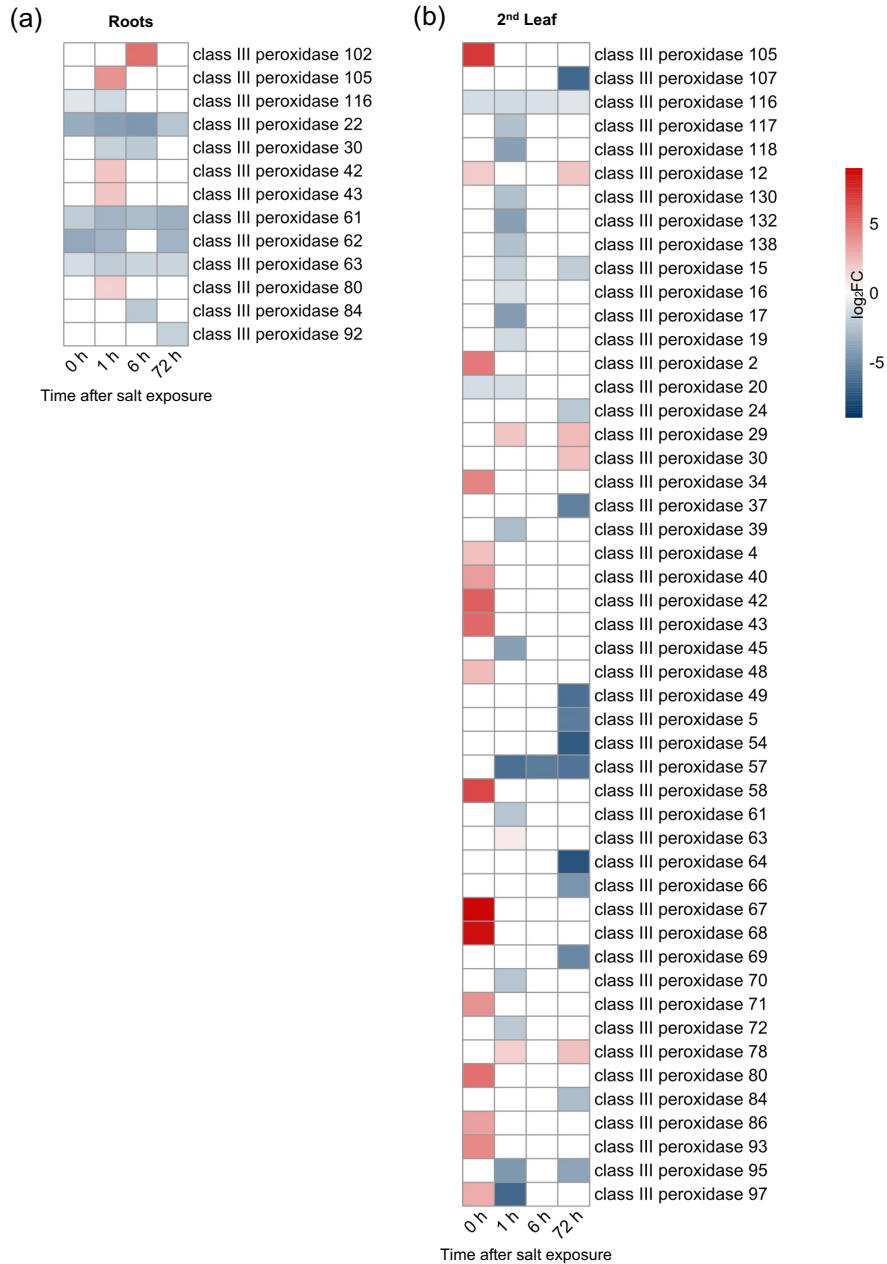


**FIGURE S5.** Kinetic expression profile of rice class III peroxidase genes displayed as heatmaps in root (a) and 2<sup>nd</sup> leaf (b).



Figure S6

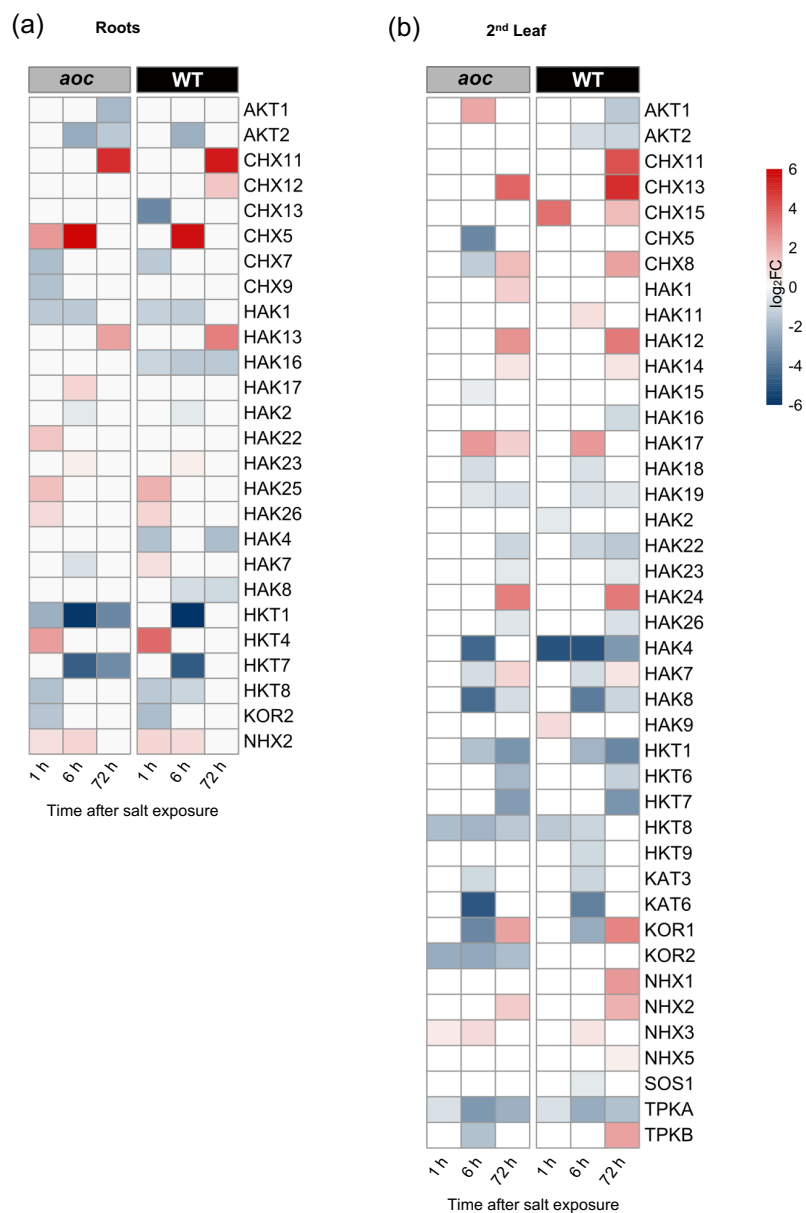


**FIGURE S6.** Kinetic expression profile of rice ion transporter genes displayed as heatmaps in root (a) and 2<sup>nd</sup> leaf (b).



Figure S7

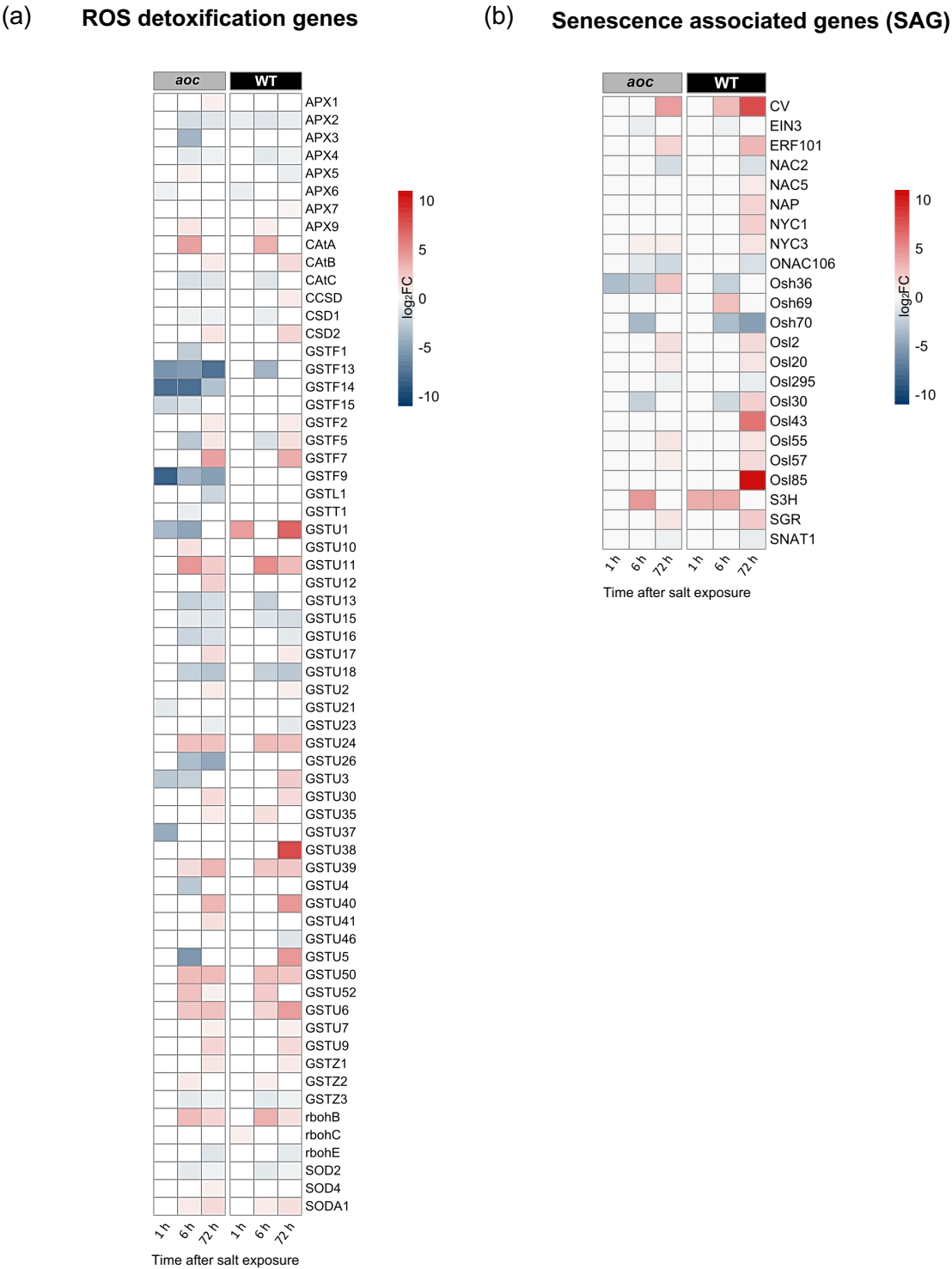
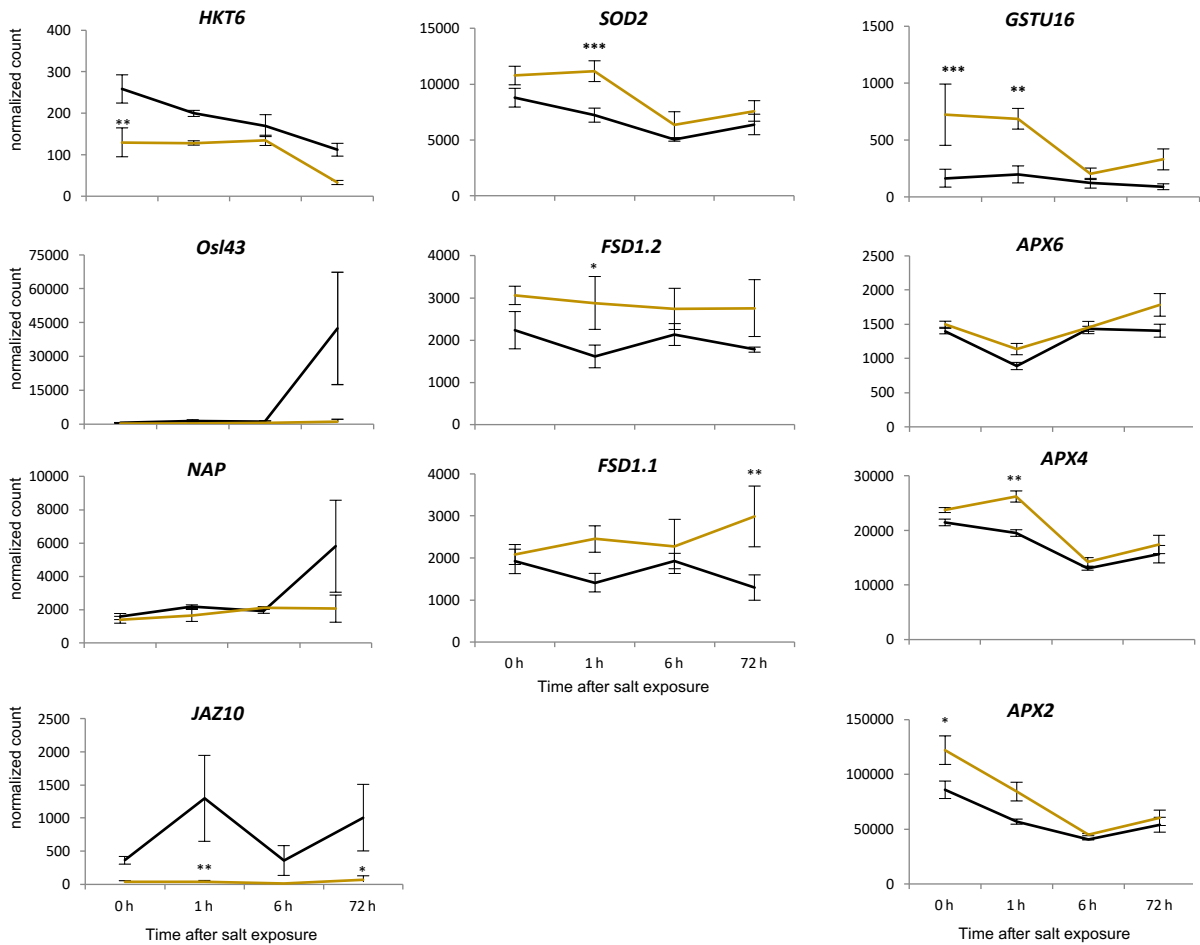


**FIGURE S7.** Kinetic expression profile of rice genes encoding ROS-scavenging or –consuming activities displayed as heatmaps in root (a) and 2<sup>nd</sup> leaf (b) of *aoc* and WT plants.



**Figure S8**

**(a) Expression profile of shoot targets in RNAseq data**



**(b) Expression profile of Roots targets in RNAseq data**

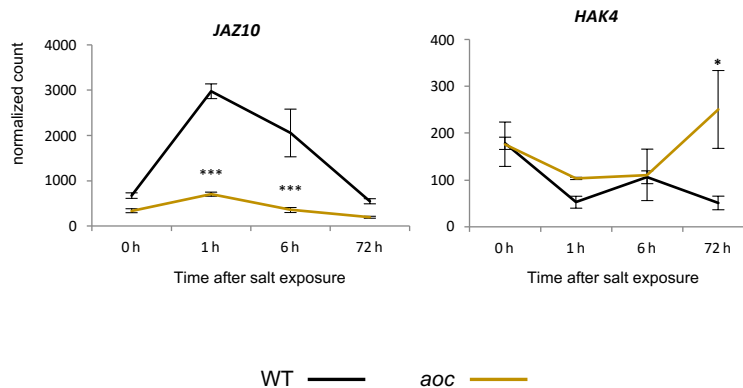


**FIGURE S8.** Kinetic expression profile of rice genes identified as probable targets of JA signaling in shoots (a) and roots (b) upon salt stress. Asterisks indicate a significant difference in means (ANOVA plus Tukey's HSD tests, \* $P < 0.05$ ; \*\* $P < 0.01$ ; \*\*\* $P < 0.001$  Student's  $t$  test \*\*\* $P < 0.001$ ).



Target	Gene ID	Forward primer	Reverse primer
UBQ5	Os01g0328400	ACCACTTCGACCGCCACTACT	ACGCCTAAGCCTGCTGGTT
UBQ10	Os02g0161900	GAGCCTCTGTTCGTCAAGTA	ACTCGATGGTCCATTAAACC
FSD1.1	Os06g0115400	TCACGTGTACTCCAGTGTGC	GCATCGGAAGCGGTTTCATC
FSD1.2	Os06g0143000	ACAACGGCAACCCATTACCA	TGGCTGCATTGATTCCCAGA
NAP	Os03g0327800	AGTTCCGCAACACCTCCA	CTGCTCGTGGTCGGAGAG
OsI43	Os01g0348900	AGGCGTGACAATCTACAG	GGTTCCAGAAATCTCCTTGA

**Table S4:** Primers used for RT-qPCR experiments.